IEEE Access
Multidisciplinary | Rapid Review | Open Access Journal

Received March 31, 2018, accepted April 18, 2018, date of publication April 25, 2018, date of current version May 16, 2018.

Digital Object Identifier 10.1109/ACCESS.2018.2829930

TAS Strategies for Incremental Cognitive MIMO Relaying: New Results and Accurate Comparison

ZAKARIA EL-MOUTAOUAKKIL[1], (Member, IEEE), KAMEL TOURKI[2], (Senior Member, IEEE), HALIM YANIKOMEROGLU[3], (Fellow, IEEE), AND SAMIR SAOUDI[1], (Senior Member, IEEE)

[1]IMT Atlantique, Lab-STICC, UBL, 29238 Brest, France
[2]Mathematical and Algorithmic Sciences Laboratory, France Research Center, Huawei Technologies France SASU, 92100 Huawei, France
[3]Department of Systems and Computer Engineering, Carleton University, Ottawa, ON K1S 5B6, Canada

Corresponding author: Zakaria El-Moutaouakkil (z.elmoutaouakkil@ieee.org)

ABSTRACT In this paper, we thoroughly elaborate on the impact different transmit-antenna selection (TAS) strategies induce in terms of the outage performance of incremental cognitive multiple-input multiple-output relaying systems employing receive maximum-ratio combining (MRC). Our setup consists of three multi-antenna secondary nodes: a transmitter, a receiver and a decode-and-forward relay node acting in a half-duplex incremental relaying mode whereas the primary transmitter and receiver are equipped with a single antenna. Only a statistical channel-state information is acquired by the secondary system transmitting nodes to adapt their transmit power. In this context, our contribution is fourfold. First, we focus on two TAS strategies that are driven by maximizing either the received signal-to-noise ratio (SNR) or signal-to-interference-plus-noise ratio (SINR), and extend their operating mode into an incremental relaying setup where MRC is carried jointly over both relaying hops. Second, given the inherited complexity, we proceed by the exact outage analysis of the direct (first-hop) transmission as a preliminary yet innovative step pertaining to the SINR-driven TAS strategy. Third, the end-to-end (second-hop) transmission outage performance is also evaluated although shown to entail an involved derivation roadmap for both TAS strategies. Fourth, we simplify our exact derivations by means of the asymptotic analysis which reveals that the detrimental effect of mutual interference on the secondary system is originated from the primary transmitter (i.e., co-channel interference) and not from the primary receiver (i.e., interference threshold). That is, even if the secondary system operates at a high tolerated amount of interference, an outage floor will still occur because the primary system will pump a high amount of co-channel interference in return. The SINR-driven TAS shows up as an optimal interference-aware strategy in this regard. It achieves the same diversity gain but a better coding gain compared to its SNR-driven counterpart. The correctness of our results is confirmed by Monte Carlo simulations and the actual outage gap between both TAS strategies is reflected.

INDEX TERMS TAS, MRC, SNR, SINR, cognitive radio, underlay, MIMO, decode-and-forward, outage probability, CSI.

I. INTRODUCTION

Driven by the ever-growing stress put on the wireless spectrum medium as a result of the huge demand on high wireless big data rates, cognitive radio (CR) has been evolving as a set of rules to cope with the spectrum under-utilization phenomenon [1]. Among these rules [2], we focus on the underlay spectrum-sharing concept as a means to allow secondary (unlicensed) users to share the same spectrum band with the primary (licensed) users. This concept has the potential of enabling the secondary users to blindly access the primary system spectrum band without any prior monitoring of its occupancy. However, as far as the interference issue is concerned, the secondary user's transmit power must be kept under a certain threshold that is predetermined by the primary system, so as to legitimately maintain its quality of service (QoS). To strike a balance in the dilemma of minimizing the engendered interference on the primary system and ensuring additional degrees of freedom in targeting its own QoS, MIMO relaying is admitted as a major breakthrough in the enhancement of the secondary system spectrum-energy efficiency. From an operator point of view, the use of relays may not be optional in situations where extending network

coverage and/or the deployment of collocated antennas is costly or infeasible. MIMO relaying can serve the secondary system in different ways. One approach is the design of cooperative beamforming or space-time block coding schemes that sort out the dilemma of coexistence on the same spectrum [3]–[5]. Inevitably, this approach requires large feedback overhead and additional complexity to compute the beamforming and precoding matrices. Furthermore, it necessitates the use of numerous radio-frequency (RF) chains to perform well.

Another approach, simple and less expensive yet realizes a good tradeoff among performance, cost and complexity, is TAS. In its simplest form, only the RF chain causing less interference on the primary system and enabling greater secondary system performance is selected. TAS has been adopted in the LTE uplink (Release 8/9) and we adopt it herein as a promising technology candidate for beyond 5G massive-oriented MIMO systems [6], [34] where spatial and index modulations will more likely be two modes of operation. If the MRC is applied at the receiver side, the technique is referred to as TAS/MRC[1] [7]. It shares the same ambition of maximizing the received SNR with the techniques literally known as maximum ratio transmission [8], [9] and transmit MRC [10] yet features the property of not relying on complete CSI feedback and all transmit RF chains.

A. RESEARCH MOTIVATION AND RELATED WORKS

In realistic cognitive spectrum sharing, the interference between the primary and secondary systems is mutual. Cross-interference mitigation using TAS/MRC has received much interest in cognitive MIMO systems whether with [11]–[14] or without [15]–[17] the use of relaying. In these works, the SNR-driven TAS strategy takes up the largest part. Besides its simplicity, it preserves, under certain ordinary conditions, the independence between the signal and interference components in the combined SINR after MRC. This independence does not always hold as it relies on the TAS strategy being opted for. Indeed, it is not preserved in the SINR-driven TAS. Having a clear understanding on the impact of the adopted TAS strategy on the combined SINR is of great importance in the secondary system outage/capacity performance analysis. In this work, we comprehensively address this challenge in incremental cognitive MIMO DF relay systems.

1) RELATED WORKS NOT USING RELAYS

The outage performance of point-to-point cognitive MIMO systems using an SNR-driven TAS have been analyzed considering both instantaneous [16] and mean-valued [15] interference constraints. With respect to the latter, i.e., when the secondary transmitter acquires a statistical CSI about its interference channel, the outage performance analysis bears resemblance with earlier works by Radaydeh on non-cognitive MIMO systems with co-channel interference (CCI) where the SNR and SINR-driven TAS strategies have initially been introduced [18]. However, to derive the system outage probability under the SINR-driven TAS, Radaydeh *et al.* [19] builds on the assumption that the per-antenna received SINRs are independent which contradicts the TAS strategy being investigated. This assumption is controversial and does only lead to an approximate outage analysis. Note that in the single receive-antenna case, the SINR-driven TAS reduces to its SNR-driven counterpart [17].

2) RELATED WORKS USING RELAYS

Very recently, cognitive MIMO relaying with TAS has received a substantial interest. In particular, Yeoh *et al.* [11] derived new expressions of the outage probability of dual-hop cognitive MIMO DF relaying using TAS/MRC and TAS/SC. In this work, the authors consider an SNR-driven TAS strategy and a negligible additive white Gaussian noise (AWGN) effect at the relay and destination nodes so as to facilitate the outage analysis. Reference [14] investigates the outage and error-rate performance of dual-hop cognitive AF relaying using an SNR-driven TAS/SC while the mutual interference between the primary and secondary systems has only been considered from one side. Alternatively, in dual-hop cognitive DF relaying with multiple single-antenna secondary destinations, Huang *et al.* [20] pointed out the importance of awareness to the primary system interference in the proposed SINR-driven scheduling algorithm. Further, in [21], the same authors addressed the impact of outdated CSI in dual-hop cognitive MIMO DF relaying using an SNR-driven TAS strategy. Very recently, AbdelNabi *et al.* partially elaborate in [22] and [23] on the SINR-driven TAS strategy for multi-hop MIMO AF relaying in a Poisson field of interferers but based on the same assumption pointed out in related works not using relays.

To the best of the authors knowledge, the SINR-driven TAS strategy has not thoroughly been analyzed for point-to-point cognitive MIMO systems while the widely used SNR-driven TAS has only been considered for dual or multi-hop cognitive MIMO DF relaying.

B. CONTRIBUTIONS

We conduct an accurate outage performance analysis of incremental cognitive MIMO DF relaying for both, the SNR and SINR-driven TAS strategies. For a better understanding of our derivation processes, the outage analysis is carried for the direct (first-hop) transmission firstly then the end-to-end (second-hop) transmission is targeted as our ultimate goal.

Our analysis for the direct transmission of our relaying scheme enriches the aforementioned related works *not* using relays with the following novel contributions:

- We conduct an exact outage analysis for the SINR-driven TAS and put previous works on the SNR-driven TAS within the same framework.

[1] If selection combining (SC) is instead applied at the receiver side, the technique is referred to as TAS/SC. According to [11], TAS/MRC performs better than TAS/SC at the expanse of an increased complexity which does not pose a real burden if the MRC is implemented at the base station level.

- We shed more light on the assumption under which the results in [19], [22], and [23] were obtained, and demonstrate that it only leads to an approximate outage analysis.
- Asymptotic closed-form expressions of our exact derivations are provided while revealing that the SINR-driven TAS achieves the same diversity gain but a better coding gain compared to its SNR-driven counterpart.
- Our results are validated by Monte Carlo simulations and interestingly show that the controversial assumption of independence among the per-transmit-antenna received SINRs gets more credibility as the multi-antenna array deployed at the secondary receiver gets larger.

Capitalizing on our results for the direct transmission, the outage performance of the end-to-end transmission resulting from the adopted relaying protocol is evaluated. Compared to the related works using relays, our contributions are:

- We extend the operating mode of both TAS strategies into an incremental relaying setup where MRC is carried jointly over both relaying hops.
- For the SNR-driven TAS, we evaluate both exactly and asymptotically the end-to-end secondary system outage performance.
- In general, the outage analysis for the SINR-driven TAS is too involved. However, we manage to evaluate the exact and asymptotic secondary system outage performance under this TAS strategy when the secondary receiver is equipped with a single antenna.
- The correctness of our findings is confirmed by Monte Carlo simulations, and the actual outage gap between both TAS strategies is reflected. The same conclusion pertaining to the achievable diversity and coding gains made for the direct transmission holds true herein as well.

The remainder of the paper is organized as follows. In Section II, we introduce our system model and power allocation methods. Then, Section III presents the adopted incremental cognitive MIMO DF relaying protocol and both TAS strategies. We address the secondary system outage performance of the direct and end-to-end transmission in Section IV and V, respectively. In Section VI, our analytical results are validated by simulations and compared for both TAS strategies before the conclusion is made in Section VII.

II. FRAMEWORK DESCRIPTION

A. SYSTEM MODEL

Our cognitive MIMO relay system consists of a secondary s_t-antenna transmitter (S-Tx) and an s_r-antenna receiver (S-Rx), both nodes share the same spectrum band with a primary single-antenna transmitter (P-Tx) and receiver (P-Rx). To ensure a highly reliable and spectrally efficient secondary system transmission, a single r_e-antenna relay node (Re) operating in a half-duplex DF incremental relaying mode is supposed to assist S-Tx in its transmission towards S-Rx. As shown in Table 1, $h_{l,k}^{a\to b}$ denotes the

TABLE 1. The coefficients $h_{l,k}^{a\to b}$ of the frequency-flat quasi-static fading channels connecting the kth transmit antenna at node of index $a \in \{p, s, r\}$ with the lth receive antenna at node of index $b \in \{p, s, r\}$.

	Receiving Node $\rightarrow$		
Transmitting Node $\downarrow$	P-Rx $(b = p)$	S-Rx $(b = s)$	Re $(b = r)$
P-Tx $(a = p)$	$h_{1,1}^{p\to p}$	$h_{l,1}^{p\to s}$	$h_{l,k}^{p\to r}$
S-Tx $(a = s)$	$h_{1,k}^{s\to p}$	$h_{l,k}^{s\to s}$	$h_{l,k}^{s\to r}$
Re $(a = r)$	$h_{1,k}^{r\to p}$	$h_{l,k}^{r\to s}$	—

coefficient of the frequency-flat fading channel connecting the kth transmit antenna at node of index $a \in \{p, s, r\}$ with the lth receive antenna at node of index $b \in \{p, s, r\}$. All channel coefficients in our cognitive MIMO relay system are assumed to be mutually independent and drawn from a zero-mean λ_{ab}-variance circularly symmetric complex Gaussian distribution. That is, $h_{l,k}^{a\to b} \sim \mathcal{CN}(0, \lambda_{ab})$. In a vector-wise form, the single-input multiple-output (SIMO) channel vector connecting the kth transmit antenna at node of index a with its respective receiving node of index b can be expressed as

$$\boldsymbol{h}_k^{i,a\to b} = \begin{bmatrix} h_{1,k}^{i,a\to b} \\ \vdots \\ h_{n,k}^{i,a\to b} \end{bmatrix} \in \mathbb{C}^{n\times 1}, \tag{1}$$

where $n = r_e$ if $b = r$ whereas $n = s_r$ if $b = s$. The exponent $i \in \{1, 2\}$ in (1) is appended to $\boldsymbol{h}_k^{a\to b}$ as long as the link $\{a \to b\}$ is involved in transmission over two consecutive relaying hops. Implicitly, we consider that our cognitive MIMO relay channel undergoes a quasi-static fading change from one relaying hop to another.

In the following, subscripts T and H denote transpose and Hermitian transpose, respectively. The cumulative distribution function (CDF) and probability distribution function (PDF) of a random vector X are denoted by $F_X(.)$ and $f_X(.)$, respectively. $|z|$ is the modulus of the complex number z while $\|z\| = \sqrt{z^H z}$ is the Frobenius norm of the complex column vector z. $\mathcal{P}(.)$, $E(.)$ and $Var(.)$ denote the probability, expectation and variance operators, respectively.

B. POWER ALLOCATION FOR S-Tx AND Re

Irrespective of the TAS criterion used by S-Tx and Re, both nodes have to keep their transmit power P under a maximum P_s and P_r, respectively, while transmitting alongside with P-Tx. Specifically, the interference caused by the secondary system at the level of the primary receiver must be limited so as not to violate its QoS. From an outage probability perspective, P_s and similarly P_r can be derived as the solution to the following system [24]–[28],

$$\begin{aligned} &\text{maximize } P \\ &\text{subject to } \begin{cases} op_p \le \varepsilon_p \\ P \le \bar{P}. \end{cases} \end{aligned} \tag{2}$$

In (2), op_p denotes the outage probability of the primary system, ε_p is an outage threshold that is defined by the

primary system to maintain its QoS, and $\bar{P}$ is a practical power maximum that neither S-Tx nor Re can exceed. For simplicity and without loss of generality, we consider that $\bar{P}$ equals the primary system transmit power P_p. The interference channel coefficients $\boldsymbol{h}_k^{i,s\to p}$ for $k \in \{1,\ldots,s_t\}$ and $\boldsymbol{h}_k^{r\to p}$ for $k \in \{1,\ldots,r_e\}$ are assumed to be completely known to P-Rx, yet S-Tx and Re can only acquire their second order statistics λ_{sp} and λ_{rp}, respectively.[2]

Proposition 1: The solution P to (2) is given by

$$P_s = \min\left\{\frac{Q_i N_0}{\lambda_{sp}}, P_p\right\}, \tag{3}$$

where

$$Q_i = \frac{P_p \lambda_{pp}}{\Phi_p N_0}\left(\frac{e^{-\frac{\Phi_p N_0}{P_p \lambda_{pp}}}}{(1-\varepsilon_p)} - 1\right) \tag{4}$$

is interpreted as the maximum tolerated interference from S-Tx at P-Rx, Φ_p is the received SINR threshold below which the primary system falls in outage, and N_0 is the AWGN at the level of P-Rx and S-Rx.

Proof: See Appendix A. ∎

The quantity Q_i must strictly be positive, i.e., the condition $e^{-\frac{\Phi_p N_0}{P_p \lambda_{pp}}} > (1-\varepsilon_p)$ in (4) must be satisfied. This means that S-Tx may stand idle with no transmission opportunity if the primary system settings are not favorable. Likewise, P_r is given by (3) where λ_{sp} is replaced by λ_{rp}.

1) FIXED INTERFERENCE THRESHOLD ($Q_i = \overline{Q}_i$)

In situations where the primary system fixes the interference threshold Q_i at a constant $\overline{Q}_i$ regardless of Φ_p, λ_{pp}, ε_p and P_p in (4), the primary system is viewed to be more selfish towards the secondary system. As a result,

$$P_s = \min\left\{\frac{\overline{Q}_i N_0}{\lambda_{sp}}, P_p\right\} \tag{5}$$

will not improve as the primary system QoS improves. Even if we operate at high primary system SNR ratios, i.e., $P_p/N_0 \to +\infty$, $\overline{Q}_i$ will be regarded as a constant that must not be exceeded anyway. This power allocation method leads to severe performance degradation of the secondary system.

2) ADAPTIVE INTERFERENCE THRESHOLD

In the opposite case, when the primary system adapts Q_i according to Φ_p, λ_{pp}, ε_p and P_p, the interference constraint put on P_s will be relaxed as P_p increases. Thus, more degrees of freedom will be given to S-Tx to transmit at a high P_s. Nevertheless, due to the spectrum sharing compromise of limiting P_s, the secondary system performance will still be impacted.

In what follows, we are more interested in scenarios where the secondary system adapts its transmit power to the primary system QoS.

[2]There exists several approaches where S-Tx and Re can obtain Q_i along with λ_{sp} (for S-Tx) and λ_{rp} (for Re) so as to adjust their transmit powers P_s and P_r, respectively. Whether Q_i is fixed (as detailed in II-B.1) or adaptive (as detailed in II-B.2), a simple time-division-based approach is to realizing perfect estimates on these parameters by P-Rx. Then, P-Rx feeds back periodically the secondary system nodes with this information via a broadcast control channel. This channel may experience a low rate which is in perfect adequacy with the fact that these parameters do not change in every channel realization, therefore no severe degradation to the primary system spectrum efficiency is induced.

III. TAS/MRC STRATEGIES FOR THE INCREMENTAL COGNITIVE MIMO DF RELAYING

A. RELAYING PROTOCOL AND COMBINED SINRs[3]

We adopt an incremental cognitive DF relaying protocol that spans one hop or at most two relaying hops if necessary [29], [32]. During the first hop, S-Tx broadcasts its symbol x_s through a given (say arbitrary chosen for now) transmit antenna $k \in \{1,\ldots,s_t\}$ while all receiving nodes S-Rx, P-Rx and Re are listening. The received baseband signals at S-Rx *before* and *after* MRC are successively given by

$$\begin{cases} \boldsymbol{y}_k^1 = \sqrt{P_s}\boldsymbol{h}_k^{1,s\to s} x_s + \sqrt{P_p}\boldsymbol{h}_1^{1,p\to s} x_p^1 + \boldsymbol{n}_s^1 \\ z_k = \boldsymbol{w}_k^H \boldsymbol{y}_k^1, \end{cases} \tag{6}$$

where $\boldsymbol{w}_k = \boldsymbol{h}_k^{1,s\to s}/\left\|\boldsymbol{h}_k^{1,s\to s}\right\| \in \mathbb{C}^{s_r\times 1}$ is the MRC weighting vector, x_p^1 is the transmitted symbol by P-Tx, and $\boldsymbol{n}_s^1$ is the AWGN noise vector at S-Rx with zero mean and variance equals to N_0 per each element. Considering that x_s and x_p^1 have zero mean and unit variance each, and that S-Rx has perfect knowledge of the channel coefficients $\boldsymbol{h}_k^{1,s\to s}$ and $\boldsymbol{h}_1^{1,p\to s}$, the conditional variance of the interference plus noise component in z_k equals to $P_p\left|\boldsymbol{w}_k^H \boldsymbol{h}_1^{1,p\to s}\right|^2 + N_0$. Therefore, the received combined SINR at S-Rx can be expressed as

$$\gamma_k^{s\to s} = \frac{P_s\left\|\boldsymbol{h}_k^{1,s\to s}\right\|^2}{P_p\dfrac{\left|\boldsymbol{h}_k^{1,s\to s^H}\boldsymbol{h}_1^{1,p\to s}\right|^2}{\left\|\boldsymbol{h}_k^{1,s\to s}\right\|^2} + N_0}. \tag{7}$$

The received SINR at Re after MRC can, following the same approach, be expressed as

$$\gamma_k^{s\to r} = \frac{P_s\left\|\boldsymbol{h}_k^{s\to r}\right\|^2}{P_p\dfrac{\left|\boldsymbol{h}_k^{s\to r^H}\boldsymbol{h}_1^{p\to r}\right|^2}{\left\|\boldsymbol{h}_k^{s\to r}\right\|^2} + N_0}. \tag{8}$$

In the case of $\gamma_k^{s\to s}$ in (7) is greater than a certain threshold Φ_s, S-Tx will move on to the next symbol transmission. Otherwise, S-Rx checks if successful decoding is detected at Re, i.e., $\gamma_k^{s\to r}$ in (8) is greater than a threshold Φ_r. If so, Re will be asked to retransmit x_s during the second hop via its selected transmit antenna. In the worst case of the link $\{s\to r\}$ connecting S-Tx with Re falls in outage, i.e., $\gamma_k^{s\to r} < \Phi_r$, S-Rx asks S-Tx to retransmit x_s instead of Re but probably through a different transmit antenna.

[3]In this Subsection, we assume that the indices k and k' in the SINRs (7), (8), (12) and (13) are arbitrary chosen. Next, Subsection III.B and Subsection III.C present the SNR and SINR-driven TAS strategies, respectively, where it becomes clear how k and k' in the aforementioned SINRs are selected.

Therefore, in the case of successful decoding at Re, the second-hop received signal at S-Rx *before* MRC is given by

$$\boldsymbol{y}_{k'}^2 = \sqrt{P_r}\boldsymbol{h}_{k'}^{r\to s}x_s + \sqrt{P_p}\boldsymbol{h}_1^{2,p\to s}x_p^2 + \boldsymbol{n}_s^2, \tag{9}$$

where $k' \in \{1,\ldots,r_e\}$ is the index of the transmit antenna used by Re while x_p^2 and $\boldsymbol{n}_s^2$ are the newly transmitted symbol by P-Tx and AWGN vector at S-Rx during the second hop, respectively. Their statistics are similar to those of x_p^1 and $\boldsymbol{n}_s^1$ in (6). Note that the secondary system transmit powers P_s and P_r are explicitly derived in the previous section. S-Rx then performs MRC over the received replicas $\boldsymbol{y}_k^1$ and $\boldsymbol{y}_{k'}^2$ during both relaying hops as if x_s was virtually sent in one shot and received by $2s_r$ receive antennas. Hence, the equivalent received signal at S-Rx after signal grouping and MRC is

$$z_{k,k'} = \boldsymbol{w}_{k,k'}^H \begin{bmatrix} \boldsymbol{y}_k^1 \\ \boldsymbol{y}_{k'}^2 \end{bmatrix} = \boldsymbol{w}_{k,k'}^H \left[\begin{bmatrix} \sqrt{P_s}\boldsymbol{h}_k^{1,s\to s} \\ \sqrt{P_r}\boldsymbol{h}_{k'}^{r\to s} \end{bmatrix} x_s + \sqrt{P_p} \begin{bmatrix} \boldsymbol{h}_1^{1,p\to s}x_p^1 \\ \boldsymbol{h}_1^{2,p\to s}x_p^2 \end{bmatrix} + \begin{bmatrix} \boldsymbol{n}_s^1 \\ \boldsymbol{n}_s^2 \end{bmatrix} \right], \tag{10}$$

where the second-hop MRC weighting vector $\boldsymbol{w}_{k,k'}$ applied on the newly built-up signal vector is constructed as

$$\boldsymbol{w}_{k,k'} = \frac{\begin{bmatrix} \boldsymbol{h}_k^{1,s\to s} \\ \boldsymbol{h}_{k'}^{r\to s} \end{bmatrix}}{\sqrt{\left\|\boldsymbol{h}_k^{1,s\to s}\right\|^2 + \left\|\boldsymbol{h}_{k'}^{r\to s}\right\|^2}}. \tag{11}$$

The indices k and k' in $z_{k,k'}$ and $\boldsymbol{w}_{k,k'}$ refer to the antennas used by S-Tx and Re during the first and second-hop transmissions, respectively. From (9) and (11), we deduce that the second-hop received SINR at S-Rx *after* MRC is given by

$$\gamma_{k,k'}^{s,r\to s} = \frac{P_s\left\|\boldsymbol{h}_k^{1,s\to s}\right\|^2 + P_r\left\|\boldsymbol{h}_{k'}^{r\to s}\right\|^2}{P_p\frac{\left|\boldsymbol{h}_k^{1,s\to s^H}\boldsymbol{h}_1^{1,p\to s} + \boldsymbol{h}_{k'}^{r\to s^H}\boldsymbol{h}_1^{2,p\to s}\right|^2}{\left\|\boldsymbol{h}_k^{1,s\to s}\right\|^2 + \left\|\boldsymbol{h}_{k'}^{r\to s}\right\|^2} + N_0}. \tag{12}$$

However, if unsuccessful decoding is detected at Re, S-Rx asks S-Tx to retransmit x_s during the second hop. In which case, the received SINR after MRC can similarly to (12) be written as

$$\gamma_{k,k'}^{s,s\to s} = \frac{P_s\left\|\boldsymbol{h}_k^{1,s\to s}\right\|^2 + P_s\left\|\boldsymbol{h}_{k'}^{2,s\to s}\right\|^2}{P_p\frac{\left|\boldsymbol{h}_k^{1,s\to s^H}\boldsymbol{h}_1^{1,p\to s} + \boldsymbol{h}_{k'}^{2,s\to s^H}\boldsymbol{h}_1^{2,p\to s}\right|^2}{\left\|\boldsymbol{h}_k^{1,s\to s}\right\|^2 + \left\|\boldsymbol{h}_{k'}^{2,s\to s}\right\|^2} + N_0}, \tag{13}$$

where k' now refers to the used antenna by S-Tx during the second hop. Finally, depending on which node Re or S-Tx is selected for retransmission, S-Rx checks if the SINR in (12) or (13) is greater than Φ_s prior to deciding if the decoding outcome is positive or negative. In the positive case, S-Tx moves on to the next symbol while, in the negative case, the protocol starts anew until successful decoding is detected.

B. SNR-DRIVEN TAS/MRC STRATEGY

The SNR-driven TAS has been widely adopted (e.g., [15]–[17], [21]) as a simple strategy that reduces to picking up k that maximizes (7) and then k' that maximizes (12) or (13) wherein all P_p is set to zero. Accordingly, the transmit antenna index k at S-Tx during the first relaying hop is selected as

$$\dot{s}_1 = \arg\max_{k\in\{1,\ldots,s_t\}}\left\{\left\|\boldsymbol{h}_k^{1,s\to s}\right\|^2\right\} \tag{14}$$

while k' is selected at Re or S-Tx depending on the selected node for retransmission as

$$\begin{cases} \dot{r} = \arg\max_{k'\in\{1,\ldots,r_e\}}\left\{\left\|\boldsymbol{h}_{k'}^{r\to s}\right\|^2\right\} \\ \dot{s}_2 = \arg\max_{k'\in\{1,\ldots,s_t\}}\left\{\left\|\boldsymbol{h}_{k'}^{2,s\to s}\right\|^2\right\}. \end{cases} \tag{15}$$

Under this TAS strategy, (7), (8), (13) and (12) should be rewritten as $\gamma_{\dot{s}_1}^{s\to s}$, $\gamma_{\dot{s}_1}^{r\to s}$, $\gamma_{\dot{s}_1,\dot{r}}^{s,r\to s}$ and $\gamma_{\dot{s}_1,\dot{s}_2}^{s,s\to s}$, respectively. Clearly, the SNR-driven TAS is not optimal in the sense that it does not take into account the interference caused by the primary system. However, it is regarded as a sub-optimal strategy realizing a reasonable complexity-performance tradeoff. We deduce from (14) and (15) that the antenna selection is disjointly carried over both relaying hops.

C. SINR-DRIVEN TAS/MRC STRATEGY

For the first time, we extend the operating mode of the SINR-driven TAS into an incremental cognitive MIMO relaying setup to optimally leverage the inherited temporal, spatial and relaying diversities. During the first hop, the index k leading to the highest $\gamma_k^{s\to s}$ is selected as

$$\ddot{s}_1 = \arg\max_{k\in\{1,\ldots,s_t\}}\left\{\gamma_k^{s\to s}\right\}. \tag{16}$$

Unlike (14) and (15), the antenna selection during the second hop is based on the combined SINR at S-Rx resulting from the combination of both received replicas of the same transmitted symbol. As a result, the selected antenna $\ddot{r}$ at Re or s_2 at S-Tx are successively given by

$$\begin{cases} \ddot{r} = \arg\max_{k'\in\{1,\ldots,r_e\}}\left\{\gamma_{\ddot{s}_1,k'}^{s,r\to s}\right\} \\ \ddot{s}_2 = \arg\max_{k'\in\{1,\ldots,s_t\}}\left\{\gamma_{\ddot{s}_1,k'}^{s,s\to s}\right\}. \end{cases} \tag{17}$$

It is worth noting here that when S-Rx is equipped with a single antenna [17], i.e., $s_r = 1$, we have $\ddot{s}_1 = \dot{s}_1$ yet the following equalities $\ddot{r} = \dot{r}$ and $\ddot{s}_2 = \dot{s}_2$ do not hold true. Under the SINR-driven TAS strategy, (7), (8), (13) and (12) should alternatively be rewritten as $\gamma_{\ddot{s}_1}^{s\to s}$, $\gamma_{\ddot{s}_1}^{r\to s}$, $\gamma_{\ddot{s}_1,\ddot{r}}^{s,r\to s}$ and $\gamma_{\ddot{s}_1,\ddot{s}_2}^{s,s\to s}$, respectively, with the difference in the number of the dots on top of the indices s_1, s_2 and r compared to the SNR-driven TAS strategy.

IV. DIRECT TRANSMISSION OUTAGE PERFORMANCE

The direct transmission of our cognitive MIMO relaying system fails in outage if $\gamma_k^{s\to s}$ is below a certain threshold Φ_s. The selected antenna k by S-Tx corresponds to $\dot{s}_1$

in (14) or $\ddot{s}_1$ in (16) depending on the adopted TAS/MRC strategy.

A. RECEIVED SINR STATISTICS FOR THE SNR-DRIVEN TAS

1) CDF OF $\gamma_{\dot{s}_1}^{s\to s}$

If S-Tx selects its transmit antenna according to (14), i.e., $k = \dot{s}_1$, the CDF of the received SINR $\gamma_{\dot{s}_1}^{s\to s}$ is given by

$$F_{\gamma_{\dot{s}_1}^{s\to s}}(\gamma) = \mathcal{P}\left(\frac{P_s X_{\dot{s}_1}^1}{P_p Z_{\dot{s}_1}^1 + N_0} < \gamma\right), \tag{18}$$

where

$$X_{\dot{s}_1}^1 = \left\| \boldsymbol{h}_{\dot{s}_1}^{1,s\to s} \right\|^2 \tag{19}$$

and

$$Z_{\dot{s}_1}^1 = \frac{\left| \boldsymbol{h}_{\dot{s}_1}^{1,s\to s^H} \boldsymbol{h}_1^{1,p\to s} \right|^2}{\left\| \boldsymbol{h}_{\dot{s}_1}^{1,s\to s} \right\|^2}. \tag{20}$$

Using the approach adopted by Shah *et al.* [30], we can prove that $X_{\dot{s}_1}^1$ and $Z_{\dot{s}_1}^1$ are independent random variables and that $Z_{\dot{s}_1}^1$ in (20) is drawn from an Exponential distribution with scale parameter equals to λ_{ps}. Note that in the particular case of S-Rx is equipped with a single antenna, the channel vectors in (19) and (20) reduce to complex scalars thus the common term between $X_{\dot{s}_1}^1$ and $Z_{\dot{s}_1}^1$, $h_{\dot{s}_1}^{1,s\to s}$, disappears from $Z_{\dot{s}_1}^1$ and the independence becomes evident. The CDF and PDF of $X_{s_1}^1$ in (19) can be expressed as

$$X_{\dot{s}_1}^1(x) = \overline{\gamma}\left(s_r, \frac{x}{\lambda_{ss}}\right)^{s_t} U(x) \tag{21}$$

and

$$f_{X_{\dot{s}_1}^1}(x) = \frac{s_t x^{s_r-1}}{\lambda_{ss}^{s_r}\Gamma(s_r)} e^{-\frac{x}{\lambda_{ss}}} \overline{\gamma}\left(s_r, \frac{x}{\lambda_{ss}}\right)^{s_t-1} U(x), \tag{22}$$

respectively, where $\overline{\gamma}(n,x) = \gamma(n,x)/\Gamma(n)$ with $\Gamma(n) = (n-1)!$ for an integer n is the regularized lower incomplete Gamma [35, Eq. 8.352.1] and $U(.)$ is the unit step function. It follows by conditioning $F_{\gamma_{\dot{s}_1}^{s\to s}}(.)$ on $Z_{\dot{s}_1}^1$ that (18) develops to

$$F_{\gamma_{\dot{s}_1}^{s\to s}}(\gamma) = \int_0^{+\infty} \overline{\gamma}\left(s_r, \frac{\gamma\left(P_p z + N_0\right)}{P_s\lambda_{ss}}\right)^{s_t} \frac{e^{-\frac{z}{\lambda_{ps}}}}{\lambda_{ps}} dz. \tag{23}$$

Lemma 1: At an early stage of our analysis, we introduce a simple yet tractable expansion of $\overline{\gamma}(l,x)$ to the power of k as follows

$$\overline{\gamma}(l,x)^k = \sum_{\substack{0\le i_1\le k \\ 0\le i_2\le i_1(l-1)}} \psi_{i_1,i_2}^{k,l} e^{-i_1 x} x^{i_2}, \tag{24}$$

where the coefficients $\psi_{i_1,i_2}^{k,l}$ for $l,k \in \mathbb{N}^*$ are governed by the following recursion

$$\begin{cases} \psi_{i_1,0}^{k,l} = \binom{k}{i_1}(-1)^{i_1}; \quad i_2 = 0 \\ \psi_{i_1,i_2}^{k,l} = \dfrac{1}{i_2}\displaystyle\sum_{i_3=1}^{\min(i_2,l-1)} \frac{(i_3 i_1 - i_2 + i_3)}{i_3!}\psi_{i_1,i_2-i_3}^{k,l}; \\ \quad 1 \le i_2 \le i_1(l-1). \end{cases} \tag{25}$$

Proof: See Appendix B. ∎

By replacing (24) into (23) and using [35, 3.382.4], the CDF of received SINR at S-Rx after MRC, $\gamma_{\dot{s}_1}^{s\to s}$, is given by

$$F_{\gamma_{\dot{s}_1}^{s\to s}}(\gamma) = \frac{e^{\frac{N_0}{P_p\lambda_{ps}}}}{\lambda_{ps}} \sum_{\substack{0\le i_1\le s_t \\ 0\le i_2\le i_1(s_r-1)}} \frac{\psi_{i_1,i_2}^{s_t,s_r}\left(\frac{\gamma P_p}{P_s\lambda_{ss}}\right)^{i_2}}{\left(\frac{i_1\gamma P_p}{P_s\lambda_{ss}} + \frac{1}{\lambda_{ps}}\right)^{i_2+1}} \times \Gamma\left(i_2+1, \frac{\gamma N_0 i_1}{P_s\lambda_{ss}} + \frac{N_0}{P_p\lambda_{ps}}\right) U(\gamma), \tag{26}$$

where $\Gamma(n,x)$ is the upper incomplete Gamma function [35, 8.352.2] for an integer n and real x.

2) PDF OF $\gamma_{\dot{s}_1}^{s\to s}$

An important consequence of deriving $F_{\gamma_{\dot{s}_1}^{s\to s}}(.)$ in (26) is that it can serve for calculating the PDF of $\gamma_{\dot{s}_1}^{s\to s}$ as $f_{\gamma_{\dot{s}_1}^{s\to s}}(\gamma) = \partial F_{\gamma_{\dot{s}_1}^{s\to s}}(\gamma)/\partial\gamma$. Using the result of Lemma 1 and [35, Eq. 8.356.4], we deduce from (23) that

$$\begin{aligned} f_{\gamma_{\dot{s}_1}^{s\to s}}(\gamma) &= s_t \int_0^{+\infty} \overline{\gamma}\left(s_r, \frac{\gamma\left(P_p z + N_0\right)}{P_s\lambda_{ss}}\right)^{s_t-1} \\ &\quad \times \frac{\partial}{\partial\gamma}\overline{\gamma}\left(s_r, \frac{\gamma\left(P_p z + N_0\right)}{P_s\lambda_{ss}}\right) \frac{e^{-\frac{z}{\lambda_{ps}}}}{\lambda_{ps}} dz \\ &= \frac{s_t e^{\frac{N_0}{P_p\lambda_{ps}}}}{\Gamma(s_r)\lambda_{ps}} \sum_{\substack{0\le i_1\le s_t-1 \\ 0\le i_2\le i_1(s_r-1)}} \frac{\psi_{i_1,i_2}^{k,l}\left(\frac{\gamma P_p}{P_s\lambda_{ss}}\right)^{i_2+s_r-1}}{\left(\frac{\gamma P_p(i_1+1)}{P_s\lambda_{ss}} + \frac{1}{\lambda_{ps}}\right)^{i_2+s_r}} \\ &\quad \times \Gamma\left(i_2+s_r, \frac{\gamma N_0(i_1+1)}{P_s\lambda_{ss}} + \frac{N_0}{P_p\lambda_{ps}}\right) U(\gamma). \end{aligned} \tag{27}$$

B. RECEIVED SINR STATISTICS FOR THE SINR-DRIVEN TAS

1) CDF OF $\gamma_{\ddot{s}_1}^{s\to s}$

If antenna $\ddot{s}_1$ at S-Tx is rather selected according to (16), the CDF of the received SINR $\gamma_{\ddot{s}_1}^{s\to s}$ after MRC is given by

$$F_{\gamma_{\ddot{s}_1}^{s\to s}}(\gamma) = \mathcal{P}\left(\frac{P_s X_{\ddot{s}_1}^1}{P_p Z_{\ddot{s}_1}^1 + N_0} < \gamma\right), \tag{28}$$

where the variables $X^1_{\ddot{s}_1} = \left\|\boldsymbol{h}^{1,s\to s}_{\ddot{s}_1}\right\|^2$ and $Z^1_{\ddot{s}_1} = \left|\boldsymbol{h}^{1,s\to s^H}_{\ddot{s}_1}\boldsymbol{h}^{1,p\to s}_1\right|^2 / \left\|\boldsymbol{h}^{1,s\to s}_{\ddot{s}_1}\right\|^2$ are constructed such as

$$\underbrace{\frac{P_s X^1_{\ddot{s}_1}}{P_p Z^1_{\ddot{s}_1} + N_0}}_{\gamma^{s\to s}_{\ddot{s}_1}} = \max_{k\in\{1,\ldots,s_t\}} \underbrace{\left\{\frac{P_s X^1_k}{P_p Z^1_k + N_0}\right\}}_{\gamma^{s\to s}_k}. \tag{29}$$

Contrary to the SNR-based TAS strategy, $X^1_{\ddot{s}_1}$ and $Z^1_{\ddot{s}_1}$ are now dependent variables whose PDFs are not known although X^1_k and Z^1_k, for a given $k \in \{1,\ldots,s_t\}$, are independent and their PDFs are known to follow Gamma and Exponential distributions, respectively. Under the assumption of independent per-transmit-antenna received SINRs (i.e., $\gamma^{s\to s}_1, \ldots, \gamma^{s\to s}_{s_t}$ are mutually independent), the CDF of $\gamma^{s\to s}_{\ddot{s}_1}$ in (29) was initially derived by Radaydeh *et al.* [19] and explored very recently in [22] and [23] as

$$F_{\gamma^{s\to s}_{\ddot{s}_1}}(\gamma) = F_{\gamma^{s\to s}_k}(\gamma)^{s_t}, \tag{30}$$

where $F_{\gamma^{s\to s}_k}(.)$ for a given $k \in \{1,\ldots,s_t\}$ is deduced from (26) by letting $s_t = 1$ before being replaced into (30).

A deeper look into $\gamma^{s\to s}_k$ in (29) especially at

$$Z^1_k = \frac{\left|\boldsymbol{h}^{1,s\to s^H}_k \boldsymbol{h}^{1,p\to s}_1\right|^2}{\left\|\boldsymbol{h}^{1,s\to s}_k\right\|^2}, \tag{31}$$

we realize that this assumption does not hold true because of the interference channel $\boldsymbol{h}^{1,p\to s}_1$ appearing across the denominator of all $\gamma^{s\to s}_k$s. Indeed, the correlation between the received SINRs is a direct outcome of applying the MRC at S-Rx despite $\boldsymbol{h}^{1,p\to s}_1$ and $\boldsymbol{h}^{1,s\to s}_k$ are being independent. Thus, (30) should consistently be rewritten as

$$F_{\gamma^{s\to s}_{\ddot{s}_1}}(\gamma) \approx F_{\gamma^{s\to s}_k}(\gamma)^{s_t} \tag{32}$$

and it becomes worth investigating whether (32) holds as a tight approximation or not. To the best of the authors knowledge, an exact derivation of (28) has not been addressed yet in the literature.

Theorem 1: The CDF in (28) of $\gamma^{s\to s}_{\ddot{s}_1}$ is given by (33), as shown at the top of the next page, where $\mathcal{U}(.,.,.)$ is the Tricomi confluent hypergeometric function [39] and the coefficients $\mathcal{A}^{s_r}_{l,n}(.,\ldots,.)$ for integers $l \in \{1,\ldots,s_t\}$ and $n \geq 0$ are calculated as in (34), as shown at the top of the next page.

Proof: See Appendix C. ∎

2) PDF OF $\gamma^{s\to s}_{\ddot{s}_1}$

As a result of Theorem 1, we state the following Corollary.

Corollary 1: The PDF of $\gamma^{s\to s}_{\ddot{s}_1}$ is given by (35), as shown at the top of the next page, where ${}_2F_1(.,.;.;.)$ is the Gauss hypergeometric function [35, Eq. 9.142] resulting from [35, Eq. 6.455.2] that, together with $\mathcal{U}(.,.,.)$, can accurately be evaluated using MATHEMATICA.

Proof: See Appendix D. ∎

We note that the derived CDF in (33) and PDF in (35) of the received SINR $\gamma^{s\to s}_{\ddot{s}_1}$ are expressed in terms of infinite series that can be shown to converge absolutely. In practice, these series are truncated to N terms (i.e., $n = 0,\ldots,N$) that are sufficient to attain an acceptable level of accuracy. A mathematical demonstration of the convergence of these series is not presented here. Nevertheless, we numerically show in Section VI that small-to-moderate values of N can lead to the desired level of accuracy in our simulation results.

C. EXACT AND ASYMPTOTIC OUTAGE ANALYSIS

We deduce from (26) and (33) that the outage performance of our system direct transmission under both TAS strategies can exactly be evaluated as

$$\begin{cases} op^1_{s,snr} = F_{\gamma^{s\to s}_{\ddot{s}_1}}(\Phi_s); & (a) \\ op^1_{s,sinr} = F_{\gamma^{s\to s}_{\ddot{s}_1}}(\Phi_s); & (b). \end{cases} \tag{36}$$

Furthermore, if S-Tx regulates its transmit power in an adaptive manner as described in Subsection II-B.2, $op^1_{s,snr}$ and $op^1_{s,sinr}$ converge to different outage probability floors, as $\frac{P_p}{N_0} \to +\infty$, that are proved in Appendix E to be equal to

$$opF^1_{s,snr} = \sum_{\substack{0\leq i_1\leq s_t \\ 0\leq i_2\leq i_1(s_r-1)}} \frac{\psi^{s_t,s_r}_{i_1,i_2}\left(\frac{\Phi_s}{\eta\lambda_{ss}}\right)^{i_2}\Gamma(i_2+1)}{\left(\frac{i_1\Phi_s}{\eta\lambda_{ss}}+\frac{1}{\lambda_{ps}}\right)^{i_2+1}} \tag{37}$$

and (38), as shown at the top of the next page, respectively, which in turn converge as $\lambda_{ps} \to 0$ to the following asymptotic expressions,

$$\begin{cases} opA^1_{s,snr} = \frac{\Gamma(s_r s_t+1)}{\Gamma(s_r+1)^{s_t}}\left(\frac{\Phi_s\lambda_{ps}}{\eta\lambda_{ss}}\right)^{s_r s_t} \\ opA^1_{s,sinr} = \frac{\sqrt{\pi}^{s_t} 2^{-2s_t\left(s_r-\frac{1}{2}\right)}\Gamma(s_r s_t+s_r)}{\Gamma(s_r)\Gamma\left(s_r+\frac{1}{2}\right)^{s_t}}\left(\frac{\Phi_s\lambda_{ps}}{\eta\lambda_{ss}}\right)^{s_r s_t}. \end{cases} \tag{39}$$

In (37), (38) and (39), the coefficient η is defined as

$$\eta = \lim_{\frac{P_p}{N_0}\to+\infty}\frac{P_s}{P_p} = \min\left\{\frac{\lambda_{pp}}{\Phi_p\lambda_{sp}}\left(\frac{\varepsilon_p}{(1-\varepsilon_p)}\right), 1\right\}. \tag{40}$$

The asymptotic closed-form expressions in (39) reveal two important conclusions:

- Even if the primary system tolerates a high amount of interference, i.e., $Q_i \to +\infty$ as a result of $P_p/N_0 \to +\infty$ according to (4) and (3), the secondary system outage performance still saturates at outage floors because the primary system pumps a high amount of co-channel interference in return, and
- The coefficient η is not inversely proportional to λ_{sp}, i.e., η does not go beyond 1 for $\lambda_{sp} \to 0$ because of the minimum operator inherited from the underlay interference constraint put on P_s. Therefore, λ_{ps} plays a more crucial role in decreasing $opA^1_{s,snr}$ and $opA^1_{s,sinr}$ in (39) than λ_{sp}.

$$F_{\gamma_{s_1}^{s\to s}}(\gamma) = \overline{\gamma}\left(s_r, \frac{\gamma N_0}{P_s\lambda_{ss}}\right)^{s_t} + \frac{1}{\Gamma(s_r)}\left(\frac{N_0}{P_p\lambda_{ps}}\right)^{s_r}\sum_{l=1}^{s_t}\binom{s_t}{l}\overline{\gamma}\left(s_r, \frac{\gamma N_0}{P_s\lambda_{ss}}\right)^{s_t-l}\frac{(-1)^{ls_r}}{\Gamma(s_r)^l}$$
$$\times e^{-\frac{\gamma N_0 l}{P_s\lambda_{ss}}}\sum_{0\le k_1,\ldots,k_l\le s_r-1}\prod_{i=1}^{l}\binom{s_r-1}{k_i}(-1)^{\sum_{i=1}^{l}k_i}\sum_{n=0}^{+\infty}\mathcal{A}_{l,n}^{s_r}(k_1,\ldots,k_l)\left(\frac{-\gamma N_0}{P_s\lambda_{ss}}\right)^{ls_r+n}$$
$$\times\Gamma\left(l+\sum_{i=1}^{l}k_i+s_r+n\right)\mathcal{U}\left(l+\sum_{i=1}^{l}k_i+s_r+n, s_r(l+1)+n+1, \frac{N_0}{P_p}\left(\frac{\gamma P_p l}{P_s\lambda_{ss}}+\frac{1}{\lambda_{ps}}\right)\right). \tag{33}$$

$$\mathcal{A}_{l,n}^{s_r}(k_1,\ldots,k_l) = (-1)^n\sum_{m_1=0}^{n}\sum_{m_2=0}^{n-m_1}\cdots\sum_{m_{l-1}=0}^{n-m_1-\cdots-m_{l-2}}\frac{1}{\prod_{i=1}^{l-1}m_i!\,(k_i+s_r+m_i)\left(k_l+s_r+n-\sum_{i=1}^{l-1}m_i\right)}. \tag{34}$$

$$f_{\gamma_{s_1}^{s\to s}}(\gamma) = \frac{s_t\left(\frac{N_0}{P_s\lambda_{ss}}\right)^{s_r}}{\Gamma(s_r-1)\,\Gamma(s_r)}\gamma^{s_r-1}e^{-\frac{\gamma N_0}{P_s\lambda_{ss}}}\overline{\gamma}\left(n_r, \frac{\gamma N_0}{P_s\lambda_{ss}}\right)^{s_t-1}\sum_{\substack{0\le i\le s_r\\0\le j\le s_r-j}}\binom{s_r}{i}\binom{s_r-i}{j}(-1)^i\left(\frac{P_p\lambda_{ps}}{N_0}\right)^{i+j}\frac{\Gamma(s_r+i+j)}{(s_r+i-1)}$$
$$\times{}_2F_1\left(1, s_r+i+j; s_r+i; -\frac{\gamma P_p\lambda_{ps}}{P_s\lambda_{ss}}\right)+\frac{s_tN_0\left(\frac{N_0}{P_p}\right)^{s_r}}{\Gamma(s_r-1)\,P_s\lambda_{ss}\lambda_{ps}^{s_r}}\sum_{l=1}^{s_t-1}\binom{s_t-1}{l}\frac{(-1)^{s_r(l+1)-1}}{\Gamma(s_r)^{l+1}}\overline{\gamma}\left(n_r, \frac{\gamma N_0}{P_s\lambda_{ss}}\right)^{s_t-1-l}$$
$$\times e^{-\frac{\gamma N_0(l+1)}{P_s\lambda_{ss}}}\sum_{\substack{0\le k\le s_r\\0\le k_1,\ldots,k_l\le s_r-1}}\binom{s_r}{k}\prod_{i=1}^{l}\binom{s_r-1}{k_i}(-1)^{\left(k+\sum_{i=1}^{l}k_i\right)}\sum_{n=0}^{+\infty}\mathcal{A}_{l+1,n}^{s_r}(k_1,\ldots,k_l,k-1)\left(\frac{-\gamma N_0}{P_s\lambda_{ss}}\right)^{(l+1)s_r+n-1}$$
$$\times\Gamma\left(l+k+\sum_{i=1}^{l}k_i+s_r+n\right)\mathcal{U}\left(l+k+\sum_{i=1}^{l}k_i+s_r+n, s_r(l+2)+n+1, \frac{N_0}{P_p}\left(\frac{\gamma(l+1)P_p}{P_s\lambda_{ss}}+\frac{1}{\lambda_{ps}}\right)\right). \tag{35}$$

$$opF_{s,sinr}^{1} = \frac{(-1)^{s_ts_r}\,e^{-\frac{\Phi_s vs_t}{\eta\lambda_{ss}}}}{\Gamma(s_r)^{s_t}}\sum_{l=1}^{s_t}\binom{s_t}{l}\sum_{0\le k_1,\ldots,k_l\le s_r-1}\prod_{i=1}^{l}\binom{s_r-1}{k_i}(-1)^{\sum_{i=1}^{l}k_i}$$
$$\times\sum_{n=0}^{+\infty}\mathcal{A}_{l,n}^{s_r}(k_1,\ldots,k_l)\left(\frac{-\Phi_s}{\eta\lambda_{ss}}\right)^{ls_r+n}\frac{\Gamma((l+1)s_r+n)}{\left(\frac{\Phi_s s_t}{\eta\lambda_{ss}}+\frac{1}{\lambda_{ps}}\right)^{(l+1)s_r+n}}. \tag{38}$$

Using the concept of generalized diversity gain [24], the achievable diversity gains (d_{snr}^1 and d_{sinr}^1) and coding gains (c_{snr}^1 and c_{sinr}^1) by the SNR and SINR-driven TAS strategies can be deduced by rewriting (39) as

$$\begin{cases} opA_{s,snr}^{1} = \left(c_{snr}^{1}/\lambda_{ps}\right)^{-d_{snr}^{1}}, \\ \Longrightarrow \begin{cases} d_{snr}^{1} = \lim_{\lambda_{ps}\to 0}\dfrac{\log opA_{s,snr}^{1}}{\log\lambda_{ps}} = s_rs_t \\ c_{snr}^{1} = \dfrac{\Gamma(s_r+1)^{\frac{1}{s_r}}}{\Gamma(s_rs_t+1)^{\frac{1}{s_rs_t}}}\dfrac{\eta\lambda_{ss}}{\Phi_s} \end{cases} \\ opA_{s,sinr}^{1} = \left(c_{sinr}^{1}/\lambda_{ps}\right)^{-d_{sinr}^{1}}, \\ \Longrightarrow \begin{cases} d_{sinr}^{1} = \lim_{\lambda_{ps}\to 0}\dfrac{\log opA_{s,sinr}^{1}}{\log\lambda_{ps}} = s_rs_t \\ c_{sinr}^{1} = \dfrac{\Gamma(s_r)^{\frac{1}{s_rs_t}}\,\Gamma\left(s_r+\frac{1}{2}\right)^{\frac{1}{s_r}}}{\pi^{\frac{1}{2s_r}}2^{\left(\frac{1}{s_r}-2\right)}\Gamma(s_rs_t+s_r)^{\frac{1}{s_rs_t}}}\dfrac{\eta\lambda_{ss}}{\Phi_s}. \end{cases} \end{cases} \tag{41}$$

As a result, both TAS strategies achieve the same diversity gain yet the SINR-driven TAS outperforms its SNR-driven counterpart in terms of the coding gain.

With this prior understanding on the direct-transmission outage performance, especially the impact of each TAS strategy on the combined SINR statistics, we embark on the end-to-end transmission outage performance of our system in the next section.

V. END-TO-END TRANSMISSION OUTAGE PERFORMANCE

Our ultimate goal in this paper is the exact derivation of the end-to-end transmission outage probability of the proposed incremental cognitive MIMO DF relaying system. Using the total probability law, it is given by [32, Eq. 7-8]

$$op_s^2 = \underbrace{\mathcal{P}\left(\gamma_k^{s\to s}<\Phi_s;\,\gamma_{k,k'}^{s,s\to s}<\Phi_s\right)}_{A_3}\underbrace{\mathcal{P}\left(\gamma_k^{s\to r}<\Phi_s\right)}_{A_1}$$
$$+\underbrace{\mathcal{P}\left(\gamma_k^{s\to s}<\Phi_s;\,\gamma_{k,k'}^{s,r\to s}<\Phi_s\right)}_{A_2}\underbrace{\mathcal{P}\left(\gamma_k^{s\to r}\ge\Phi_s\right)}_{1-A_1}, \tag{42}$$

where k and k' are selected depending on the TAS/MRC strategy being adopted during both relaying hops.

A. DERIVATION OF A_1 AND A_3

Due to the independence between the random channel vectors $\boldsymbol{h}_k^{1,s\to s}$ and $\boldsymbol{h}_k^{s\to r}$ for $k \in \{1,\ldots,s_t\}$, the TAS criterion used by S-Tx does not impact the derivation of A_1 in (42). That is, the channel connecting S-Tx and Re is regarded as a SIMO channel. Therefore, A_1 can be deduced from (26) as

$$A_1 = F_{\gamma_{\dot{s}_1}^{s\to s}}(\Phi_s) \tag{43}$$

after making the following change of parameters $\lambda_{ss} = \lambda_{sr}$, $\lambda_{ps} = \lambda_{pr}$, $s_t = 1$ and finally $s_r = r_e$.

As for the probability A_3 in (42), it is viewed as a particular case of A_2 since

$$A_3 = A_2 \tag{44}$$

when $r_e = s_t$, $\lambda_{rs} = \lambda_{ss}$ and $\lambda_{rp} = \lambda_{sp}$. The latter equality implies that $P_r = P_s$. Hence, we proceed with the derivation of A_2 according to both TAS/MRC strategies for an arbitrary r_e, λ_{rs} and λ_{rp}. Then, we deduce A_3 from the final expression of A_2 by making the aforementioned change of parameters.

B. DERIVATION OF A_2 FOR THE SNR-DRIVEN TAS/MRC STRATEGY

According to (14) and (15), $A_2 = \dot{A}_2$ can be expressed as

$$\dot{A}_2 = \mathcal{P}\left(\frac{P_s X_{\dot{s}_1}^1}{P_p Z_{\dot{s}_1}^1 + N_0} < \Phi_s;\ \frac{P_s X_{\dot{s}_1}^1 + P_r X_{\dot{r}}}{P_p Z_{\dot{s}_1,\dot{r}}^2 + N_0} < \Phi_s\right), \tag{45}$$

where $X_{\dot{s}_1}^1$ given by (19) and $X_{\dot{r}} = \left\|\boldsymbol{h}_{\dot{r}}^{r\to s}\right\|^2$ are independent but not identically distributed variables. The CDF of $X_{\dot{r}}$ is given by (21) where s_t and λ_{ss} are being replaced by r_e and λ_{rs}, respectively. On the contrary, $Z_{\dot{s}_1}^1$ in (20) and

$$Z_{\dot{s}_1,\dot{r}}^2 = \frac{\left|\boldsymbol{h}_{\dot{s}_1}^{1,s\to s^H}\boldsymbol{h}_1^{1,p\to s} + \boldsymbol{h}_{\dot{r}}^{r\to s^H}\boldsymbol{h}_1^{2,p\to s}\right|^2}{\left\|\boldsymbol{h}_{\dot{s}_1}^{1,s\to s}\right\|^2 + \left\|\boldsymbol{h}_{\dot{r}}^{r\to s}\right\|^2} \tag{46}$$

are dependent yet identically distributed λ_{sp}-mean Exponential variables. Given the distribution of the marginals, it is not necessarily true to deduce that the joint PDF of $Z_{\dot{s}_1}^1$ and $Z_{\dot{s}_1,\dot{r}}^2$ follows a bivariate Exponential distribution. Indeed, this implication does not hold true in our case of study. However, conditioned on $\boldsymbol{h}_{\dot{s}_1}^{1,s\to s}$ and $\boldsymbol{h}_{\dot{r}}^{r\to s}$, the generating complex Gaussian variables of $Z_{\dot{s}_1}^1$,

$$\frac{\boldsymbol{h}_{\dot{s}_1}^{1,s\to s^H}\boldsymbol{h}_1^{1,p\to s}}{\left\|\boldsymbol{h}_{\dot{s}_1}^{1,s\to s}\right\|}, \tag{47}$$

and $Z_{\dot{s}_1,\dot{r}}^2$,

$$\frac{\boldsymbol{h}_{\dot{s}_1}^{1,s\to s}\boldsymbol{h}_1^{1,p\to s} + \boldsymbol{h}_{\dot{r}}^{r\to s}\boldsymbol{h}_1^{2,p\to s}}{\sqrt{\left\|\boldsymbol{h}_{\dot{s}_1}^{1,s\to s}\right\|^2 + \left\|\boldsymbol{h}_{\dot{r}}^{r\to s}\right\|^2}}, \tag{48}$$

appear to arise from nonsingular linear combinations of independent Gaussian variables. Therefore, they jointly follow a bivariate complex Gaussian distribution. As a result, the joint PDF of $Z_{\dot{s}_1}^1$ and $Z_{\dot{s}_1,\dot{r}}^2$ conditioned on $X_{\dot{s}_1}^1 = x_1$ and $X_{\dot{r}} = x_2$ is a bivariate Exponential distribution that is given by

$$f_{Z_{\dot{s}_1}^1, Z_{\dot{s}_1,\dot{r}}^2 \mid x_1,x_2}(z_1,z_2) = \frac{e^{-\frac{(z_1+z_2)}{\lambda_{ps}(1-\rho_x^2)}}}{\lambda_{ps}^2\left(1-\rho_x^2\right)} I_0\left(\frac{2\rho_x\sqrt{z_1 z_2}}{\lambda_{ps}\left(1-\rho_x^2\right)}\right) \times U(z_1)U(z_2), \tag{49}$$

where ρ_x squared is the correlation coefficient between $Z_{\dot{s}_1}^1$ and $Z_{\dot{s}_1,\dot{r}}^2$ conditioned on $X_{\dot{s}_1}^1 = x_1$ and $X_{\dot{r}} = x_2$, and $I_0(.)$ is the zeroth-order modified Bessel function of the first kind whose series expansion equals

$$I_0(z) = \sum_{i=0}^{+\infty} \frac{\left(\frac{1}{4}z^2\right)^i}{i!^2}. \tag{50}$$

Lemma 2: The correlation coefficient between $Z_{\dot{s}_1}^1$ and $Z_{\dot{s}_1,\dot{r}}^2$ conditioned on $X_{\dot{s}_1}^1 = x_1$ and $X_{\dot{r}} = x_2$ is given by $\rho_x^2 = \frac{x_1}{x_1+x_2}$ while its averaged variant $\rho^2 = E\left[X_{\dot{s}_1}^1 / \left(X_{\dot{s}_1}^1 + X_{\dot{r}}\right)\right]$ can be expressed as in (51), as shown at the top of the next page.[4]

Proof: See Appendix F. ∎

We proceed now with the derivation of $\dot{A}_2$ starting from equation (45). It can be rewritten as

$$\dot{A}_2 = \iiiint_{\mathcal{R}} f_{Z_{\dot{s}_1}^1, Z_{\dot{s}_1,\dot{r}}^2 \mid x_1,x_2}(z_1,z_2) f_{X_{\dot{r}}}(x_2) f_{X_{\dot{s}_1}^1}(x_1) \times dx_1 dx_2 dz_1 dz_2 \tag{52}$$

$$= \frac{s_t r_e}{(\lambda_{ss}\lambda_{rs})^{s_r}\,\Gamma(s_r)^2}\left[\mathcal{I}_{\mathcal{R}_1} + \mathcal{I}_{\mathcal{R}_2} + \sum_{i=0}^{+\infty}\frac{\mathcal{I}_{\mathcal{R}_3}(i)}{i!^2}\right], \tag{53}$$

where $\mathcal{R} = \{\mathcal{R}_1 \cup \mathcal{R}_2 \cup \mathcal{R}_3\}$ is our four-dimensional integration region that can be subdivided into three distinct subregions as

$$\begin{cases} \mathcal{R}_1 = \left\{(x_1,x_2,z_1,z_2) \in \mathbb{R}^{+4} \mid 0 < x_1 < \beta,\ 0 < x_2 < \frac{1}{\delta}(\beta - x1), 0 < z_1, 0 < z_2\right\} \\ \mathcal{R}_2 = \left\{(x_1,x_2,z_1,z_2) \in \mathbb{R}^{+4} \mid 0 < x_1 < \beta,\ \frac{1}{\delta}(\beta - x1) < x_2, 0 < z_1,\ \frac{1}{\alpha}(-\beta + x_1 + \delta x_2) < z_2\right\} \\ \mathcal{R}_3 = \left\{(x_1,x_2,z_1,z_2) \in \mathbb{R}^{+4} \mid \beta < x_1,\ 0 < x_2, \frac{1}{\alpha}(-\beta + x_1) < z_1,\ \frac{1}{\alpha}(-\beta + x_1 + \delta x_2) < z_2\right\} \end{cases} \tag{54}$$

[4] In the particular case of $X_{\dot{s}_1}^1$ and $X_{\dot{r}}^2$ are identically distributed in addition to being independent, we would have easily obtained $\rho^2 = E\left[X_{\dot{s}_1}^1 / \left(X_{\dot{s}_1}^1 + X_{\dot{r}}\right)\right] = E\left[X_{\dot{r}} / \left(X_{\dot{r}} + X_{\dot{s}_1}^1\right)\right] = \frac{1}{2}$ compared to the general expression (51). This case arises in the calculation of A_3 in (42) reflecting the event in which S-Tx transmits during both relaying hops.

$$\rho^2 = \frac{s_t r_e}{\Gamma(s_r)^2} \sum_{\substack{0\le i_1\le n_t-1\\ 0\le i_2\le i_1(n_r-1)}} \frac{\psi_{i_1,i_2}^{s_t-1,s_r}}{\lambda_{ss}^{i_2+s_t}} \Gamma(s_r+i_2+1) \sum_{\substack{0\le i_3\le r_e-1\\ 0\le i_4\le i_1(s_r-1)}} \frac{\psi_{i_3,i_4}^{r_e-1,s_r}}{\lambda_{rs}^{i_4+s_r}} \frac{\Gamma(s_r+i_4)}{(2s_r+i_2+i_4)} \times \frac{1}{\left(\frac{i_3+1}{\lambda_{rs}}\right)^{2s_r+i_2+i_4}} {}_2F_1\left(s_r+i_2+1, 2s_r+i_2+i_4; 2s_r+i_2+i_4+1; 1-\frac{\lambda_{rs}(i_1+1)}{\lambda_{ss}(i_3+1)}\right). \quad (51)$$

$$\mathcal{I}_{\mathcal{R}_1} = \sum_{\substack{0\le i_1\le s_t-1\\ 0\le i_2\le i_1(s_r-1)}} \frac{\psi_{i_1,i_2}^{s_t-1,s_r}}{\lambda_{ss}^{i_2}} \sum_{\substack{0\le i_3\le r_e-1\\ 0\le i_4\le i_3(s_r-1)}} \frac{\psi_{i_3,i_4}^{r_e-1,s_r}}{\lambda_{rs}^{i_4}} \frac{\Gamma(s_r+i_4)\Gamma(s_r+i_2)}{\left(\frac{i_3+1}{\lambda_{rs}}\right)^{s_r+i_4}} \left[\left(\frac{\lambda_{ss}}{i_1+1}\right)^{s_r+i_2} \overline{\gamma}\left(s_r+i_2, \frac{(i_1+1)\beta}{\lambda_{ss}}\right) - e^{-\frac{\beta(i_3+1)}{\lambda_{rs}\delta}} \sum_{m=0}^{s_r+i_4-1} \left(\frac{i_3+1}{\lambda_{rs}\delta}\right)^m \beta^{s_r+i_2+m} \Gamma(m+1)\, {}_1F_1\left(s_r+i_2; s_r+i_2+m+1; \beta\left(\frac{i_3+1}{\lambda_{rs}\delta}-\frac{i_1+1}{\lambda_{ss}}\right)\right)\right]. \quad (56)$$

$$\mathcal{I}_{\mathcal{R}_2} = \sum_{\substack{0\le i_1\le s_t-1\\ 0\le i_2\le i_1(s_r-1)}} \frac{\psi_{i_1,i_2}^{s_t-1,s_r}}{\lambda_{ss}^{i_2}} \sum_{\substack{0\le i_3\le r_e-1\\ 0\le i_4\le i_3(s_r-1)}} \frac{\psi_{i_3,i_4}^{r_e-1,s_r}}{\lambda_{rs}^{i_4}} \frac{\Gamma(s_r+i_4)\Gamma(s_r+i_2)}{\left(\frac{i_3+1}{\lambda_{rs}}+\frac{\delta}{\lambda_{ps}\alpha}\right)^{s_r+i_4}} e^{-\beta\left(\frac{i_3+1}{\lambda_{rs}\delta}+\frac{1}{\lambda_{ps}\alpha}\right)} \sum_{m=0}^{s_r+i_4-1} \Gamma(m+1) \times \left(\frac{i_3+1}{\lambda_{rs}\delta}+\frac{1}{\lambda_{ps}\alpha}\right)^m \beta^{s_r+i_2+m} {}_1F_1\left(s_r+i_2; s_r+i_2+m+1; \beta\left(\frac{i_3+1}{\lambda_{rs}\delta}-\frac{i_1+1}{\lambda_{ss}}\right)\right). \quad (57)$$

$$\mathcal{I}_{\mathcal{R}_3}(i) = \sum_{\substack{0\le i_1\le s_t-1\\ 0\le i_2\le i_1(s_r-1)}} \frac{\psi_{i_1,i_2}^{s_t-1,s_r}}{\lambda_{ss}^{i_2}} \sum_{\substack{0\le i_3\le r_e-1\\ 0\le i_4\le i_3(s_r-1)}} \frac{\psi_{i_3,i_4}^{r_e-1,s_r}}{\lambda_{rs}^{i_4}} \sum_{u=0}^{i}\sum_{v=0}^{i} \frac{i!^2}{u!v!\left(\lambda_{ps}\alpha\right)^{u+v}} e^{\frac{2\beta}{\lambda_{ps}\alpha}} \sum_{w=0}^{v} \binom{v}{w} \delta^w \times \int_{\beta}^{+\infty} x_1^{s_r-1+i+i_2} (-\beta+x_1)^{v+u-w} e^{-\left(\frac{(i_1+1)}{\lambda_{ss}}+\frac{2+\delta}{\lambda_{ps}\alpha}\right)x_1} \int_0^{+\infty} \frac{x_2^{s_r+i_4+w-u-v}}{(x_1+x_2)^{i+1-u-v}} e^{-\left(\frac{(i_3+1)}{\lambda_{rs}}+\frac{\delta}{\lambda_{ps}\alpha}\right)x_2} e^{-\frac{2x_1(-\beta+x_1)}{\lambda_{ps}\alpha x_2}} dx_2 dx_1. \quad (58)$$

$$\ddot{A}_2 = \int_0^{+\infty} \int_0^{\frac{\Phi_s}{P_s}(P_p z+N_0)} \underbrace{\mathcal{P}\left(\frac{P_s x+P_r X_1}{P_p Z_{\ddot{s}_1,1}^2|x,z+N_0} < \Phi_s; \ldots; \frac{P_s x+P_r X_{r_e}}{P_p Z_{\ddot{s}_1,r_e}^2|x,z+N_0} < \Phi_s\right)}_{\ddot{A}_2(x,z)} f_{X_{\ddot{s}_1}^1, Z_{\ddot{s}_1}^1}(x,z)\, dxdz. \quad (61)$$

over each the integral in (52) will be carried on. In (54), $\alpha = \frac{\Phi_s P_p}{P_s}$, $\beta = \frac{\Phi_s N_0}{P_s}$ and $\delta = \frac{P_r}{P_s}$. Given (22), the first quadruple integral $\mathcal{I}_{\mathcal{R}_1}$ over the region $\mathcal{R}_1$ in (53) can be expressed as

$$\mathcal{I}_{\mathcal{R}_1} = \int_0^{\beta} \int_0^{\frac{1}{\delta}(\beta-x1)} (x_1 x_2)^{s_r-1} e^{-\frac{x_1}{\lambda_{ss}}-\frac{x_2}{\lambda_{rs}}} \times \overline{\gamma}\left(s_r, \frac{x_1}{\lambda_{ss}}\right)^{s_t-1} \overline{\gamma}\left(s_r, \frac{x_2}{\lambda_{rs}}\right)^{r_e-1} dx_2 dx_1. \quad (55)$$

It can further be developed using the result of Lemma 1, [35, Eq. 3.351.1] and [35, Eq. 3.383.1] to obtain (56), as shown at the top of this page, where ${}_1F_1(.;.;.)$ denotes the Kummer confluent hypergeometric function [35, Eq. 9.210.1]. Following the same steps, $\mathcal{I}_{\mathcal{R}_2}$ and $\mathcal{I}_{\mathcal{R}_3}(i)$ can also be derived using [35, Eq. 3.351.2] (instead of [35, Eq. 3.351.1] for the derivation of $\mathcal{I}_{\mathcal{R}_1}$), (49) and [35, Eq. 8.352.2] as (57) and (58), as shown at the top of this page, respectively. To the best of the authors knowledge, the double integral in (58) cannot be resolved in closed form. Therefore, we resort to its accurate numerical integration using MATHEMATICA.

At this stage, we conclude with the derivation of $\dot{A}_2$ then $\dot{A}_3$ in (44) for the SNR-driven TAS/MRC strategy and consequently the derivation of the end-to-end transmission outage probability (42) of our incremental cognitive MIMO DF relay system under this TAS strategy.

C. DERIVATION OF A_2 FOR THE SINR-DRIVEN TAS/MRC STRATEGY

It follows from the SINR-driven TAS/MRC criterion proposed in (16) and (17), that $A_2 = \ddot{A}_2$ and

$$\ddot{A}_2 = \mathcal{P}\left(\frac{P_s X_{\ddot{s}_1}^1}{P_p Z_{\ddot{s}_1}^1 + N_0} < \Phi_s; \frac{P_s X_{\ddot{s}_1}^1 + P_r X_{\ddot{r}}}{P_p Z_{\ddot{s}_1,\ddot{r}}^2 + N_0} < \Phi_s\right). \quad (59)$$

The derivation of $\ddot{A}_2$ is too involved because of the correlation linking most the variables in (59). A summary of the relationship between all pairs of variables in our system is shown in Table 2. Despite, we develop $\ddot{A}_2$ in a general integral format, then to get much intuition into its exact derivation, we proceed by considering the particular case of single receive-antenna at S-Rx, i.e., $s_r = 1$.

The right-hand side event of (59) can be rewritten as

$$\frac{P_s X_{\ddot{s}_1}^1 + P_r X_{\ddot{r}}}{P_p Z_{\ddot{s}_1,\ddot{r}}^2 + N_0} = \max_{k\in\{1,\ldots,r_e\}} \left\{\frac{P_s X_{\ddot{s}_1}^1 + P_r X_k}{P_p Z_{\ddot{s}_1,k}^2 + N_0}\right\}. \quad (60)$$

TABLE 2. The relationship between each two variables resulting from the use of both TAS/MRC strategies. $\perp$ and $\propto$ denote for the independence and dependence, respectively.

Variables		SNR-driven TAS ($s_i = \dot{s}_i, r = \dot{r}$)	SINR-driven TAS ($s_i = \ddot{s}_i, r = \ddot{r}$)
$X^1_{s_1}$	$X^2_{s_2}$	$\perp$	$\propto$
$X^1_{s_1}$	$Z^1_{s_1}$	$\perp$	$\propto$
$X^1_{s_1}$	$Z^2_{s_1,r}$ or $Z^2_{s_1,s_2}$	$\perp$	$\propto$
$X^2_{s_2}$	$Z^1_{s_1}$	$\perp$	$\propto$
$X^2_{s_2}$	$Z^2_{s_1,r}$ or $Z^2_{s_1,s_2}$	$\perp$	$\propto$
$Z^1_{s_1}$	$Z^2_{s_1,r}$or $Z^2_{s_1,s_2}$	$\propto$	$\propto$

To expand $\ddot{A}_2$, we condition both events in (59) on $X^1_{\ddot{s}_1}$ and $Z^1_{\ddot{s}_1}$. Consequently, we obtain (61), as shown at the top of the previous page, where the conditional probability $\ddot{A}_2(x,z)$ can in turn be expressed as

$$\ddot{A}_2(x,z) = \int_0^{+\infty} \mathcal{P}\left(\frac{P_s x + P_r X_k}{P_p \frac{Z^2_{\ddot{s}_1,k}|x,z,v}{x+X_k} + N_0} < \Phi_s \right)^{r_e} f_V(v)\, dv, \tag{62}$$

where $V = \left\| \boldsymbol{h}^{2,p\to s} \right\|^2$. Expression (62) has resulted from applying the same approach used in Subsection IV-B. In (62), the variable $Z^2_{\ddot{s}_1,k}|x,z,v$ for $k \in \{1,\ldots,r_e\}$ is given by

$$Z^2_{\ddot{s}_1,k}|x,z,v = \left| \sqrt{xz} + \boldsymbol{h}_k^{r\to s^H} \boldsymbol{h}_1^{2,p\to s} e^{-\mathrm{i}\theta} \right|^2 v, \tag{63}$$

where the random variable θ corresponds to the argument of $\boldsymbol{h}^{1,s\to s^H}_{\ddot{s}_1} \boldsymbol{h}^{1,p\to s}$ that is independent of $\boldsymbol{h}_k^{r\to s^H} \boldsymbol{h}_1^{2,p\to s}$. After being properly scaled, it turns out that $Z^2_{\ddot{s}_1,k}|x,z,v$ follows a non-central Chi-squared distribution. Therefore, the derivation of $\ddot{A}_2(x,z)$ involves knowing the bivariate PDF of $2X_k/\lambda_{rs}$ and $2Z^2_{\ddot{s}_1,k}|x,z,v/v\lambda_{rs}$ as central and non-central chi-squared random variables, respectively, with different degrees of freedom and noncentrality parameters. To the best of our knowledge, the bivariate PDF in question has not been derived yet in the literature. As a starting point, we resort to the single receive-antenna case at S-Rx in order to get some insights into the derivation of $\ddot{A}_2$ in (59) as the latter appears to be too complex to evaluate for an arbitrary s_r.

Theorem 2: The bivariate PDF of X_k and $Z^2_{\ddot{s}_1,k}|x,z,v$ in the case of an arbitrary non-negative reals x, z and v, and $s_r = 1$ is given by

$$f_{X_k, Z^2_{\ddot{s}_1,k}|x,z,v}(x_2,z_2) = \begin{cases} \dfrac{e^{-x_2/\lambda_{rs}}}{\lambda_{rs}\pi\sqrt{4xzx_2v - (z_2-(xz+x_2v))^2}}; \\ \qquad \left(\sqrt{xz}-\sqrt{x_2v}\right)^2 < z_2 < \left(\sqrt{xz}+\sqrt{x_2v}\right)^2 \\ 0; \quad \text{Otherwise.} \end{cases} \tag{64}$$

Proof: See Appendix G. ■

Note that the joint PDF in (61), $f_{X^1_{\ddot{s}_1}, Z^1_{\ddot{s}_1}}(.,.)$, now reduces for $s_r = 1$, $x \geq 0$ and $z \geq 0$ to

$$f_{X^1_{\ddot{s}_1}, Z^1_{\ddot{s}_1}}(x,z) = s_t \left(1 - e^{-\frac{x}{\lambda_{ss}}}\right)^{s_t - 1} \frac{e^{-\frac{x}{\lambda_{ss}}}}{\lambda_{ss}} \frac{e^{-\frac{z}{\lambda_{ps}}}}{\lambda_{ps}} \tag{65}$$

because both variables $X^1_{\ddot{s}_1}$ and $Z^1_{\ddot{s}_1}$ becomes independent. Let the probability inside (62) before raised to the power of r_e be denoted by $\ddot{A}_2(x,z,v)$. As a result of Theorem 2, it can now be expressed as

$$\ddot{A}_2(x,z,v) = \iint_{\mathcal{T}} f_{X_k, Z^2_{\ddot{s}_1,k}|x,z,v}(x_2,z_2)\, dx_2 dz_2, \tag{66}$$

where $\mathcal{T} = \{\mathcal{T}_1 \cup \mathcal{T}_2 \cup \mathcal{T}_3\}$ is a two-dimensional region that, for a given $z \geq 0$ and $0 \leq x \leq \Phi_s\left(P_p z + N_0\right)/P_s$, defines the sub-regions over which the inequality $(P_s x + P_r x_2 - \Phi_s N_0) \leq z_2 \Phi_s P_p / (x + x_2)$ holds true. It can be divided into three distinct sub-regions

$$\begin{cases} \mathcal{T}_1 = \left\{ (x_2,z_2) \in \mathbb{R}^{+2} \,|\, 0 \leq z, 0 \leq x \leq \beta, \right. \\ \qquad \left. 0 \leq x_2 \leq \frac{1}{\delta}(\beta - x), 0 \leq z_2 \right\} \\ \mathcal{T}_2 = \left\{ (x_2,z_2) \in \mathbb{R}^{+2} \,|\, 0 \leq z, 0 \leq x \leq \beta, \right. \\ \qquad \left. \frac{1}{\delta}(\beta - x) < x_2, \frac{1}{\alpha}(-\beta + x_1 + \delta x_2) < z_2 \right\} \\ \mathcal{T}_3 = \left\{ (x_2,z_2) \in \mathbb{R}^{+2} \,|\, 0 \leq z, \beta < x \leq \beta + \alpha z \right. \\ \qquad \left. 0 \leq x_2, \frac{1}{\alpha}(-\beta + x + \delta x_2) < z_2 \right\}, \end{cases} \tag{67}$$

where the parameters α, β and δ are similarly defined as in the previous section. Note that it becomes not trivial to precise $\mathcal{T}$ if we add the definition domain of the bivariate distribution in (64) to the system of inequalities (67) as it will involve solving quartic inequalities. Indeed, we replace (64) as is into (66) and carry out the double integration over $\mathcal{T}_1$, $\mathcal{T}_2$ and $\mathcal{T}_3$. After usual mathematical manipulation, we derive $\ddot{A}_2(x,z,v)$ as shown in (68), as shown at the top of the next page, where the function $\mathcal{G}(.)$ is given by

$$\mathcal{G}(u) = \begin{cases} 1; & u \leq -1 \\ \frac{1}{\pi}\arccos(u); & -1 < u < 1 \\ 0; & \text{Otherwise.} \end{cases} \tag{69}$$

Finally, we substitute (68) into $\ddot{A}_2(x,z)$ which in turn, raised to the power of r_e, is substituted into (61). The resulting expression of $\ddot{A}_2$ is a three-dimensional integration over v, x and z, successively, without counting the integral over x_2 in (68). Clearly, it is difficult to evaluate $\ddot{A}_2$ in a closed form for the SINR-driven TAS/MRC strategy even in the single receive antenna case at S-Rx.

$$\ddot{A}_2(x,z,v)=\begin{cases}\left(1-e^{-\frac{1}{\delta}(\beta-x)}\right)+\int\limits_{\frac{1}{\delta}(\beta-x)}^{+\infty}\frac{e^{-\frac{x_2}{\lambda_{rs}}}}{\lambda_{rs}}\mathcal{G}\left(\frac{(-\beta+x+\delta x_2)-\alpha\,(xz+x_2v)}{2\alpha\sqrt{xzvx_2}}\right)dx_2; & 0\le x\le\beta\\ \int\limits_0^{+\infty}\frac{e^{-\frac{x_2}{\lambda_{rs}}}}{\lambda_{rs}}\mathcal{G}\left(\frac{(-\beta+x+\delta x_2)\,(x+x_2)-\alpha\,(xz+x_2v)}{2\alpha\sqrt{xzvx_2}}\right)dx_2; & \beta<x\le\beta+\alpha z\\ 0; & \text{Otherwise.}\end{cases}\tag{68}$$

D. EXACT AND ASYMPTOTIC OUTAGE ANALYSIS

Depending on the adopted TAS strategy, we replace A_2 and A_3 by $\dot{A}_2$ and $\dot{A}_3$ or $\ddot{A}_2$ and $\ddot{A}_3$ into (42) to evaluate the end-to-end outage probability of our incremental cognitive MIMO DF relaying system as

$$\begin{cases}op^2_{s,snr}=\dot{A}_3A_1+\dot{A}_2\,(1-A_1); & (a)\\ op^2_{s,sinr}=\ddot{A}_3A_1+\ddot{A}_2\,(1-A_1); & (b)\end{cases}\tag{70}$$

for the SNR and SINR-driven TAS/MRC strategies, respectively. The outage probability floors $opF^2_{s,snr}$ and $opF^2_{s,sinr}$ can be deduced from the final expressions of $op^2_{s,snr}$ and $op^2_{s,sinr}$ in (70) as $P_p/N_0\to+\infty$, respectively, by setting $\alpha=\Phi_s/\eta$, $\beta=0$ and $\delta=\frac{\kappa}{\eta}$ where κ is given by η in (40) with λ_{sp} is being replaced by λ_{rp}. Following the approach used to derive the asymptotic expressions of the direct-transmission outage probability, (70), as $\lambda_{ps}\to0$, can be approximated by

$$\begin{cases}opA^2_{s,snr}\approx\dot{A}_2=\left(\frac{c^2_{snr}}{\lambda_{ps}}\right)^{-d^2_{snr}}\\ opA^2_{s,sinr}\approx\ddot{A}_2=\left(\frac{c^2_{sinr}}{\lambda_{ps}}\right)^{-d^2_{sinr}},\end{cases}\tag{71}$$

where $d^2_{snr}=s_r\,(s_t+r_e)$ is the generalized diversity gain achieved by the SNR-driven TAS while $d^2_{sinr}=(s_t+r_e)$ is that achieved by the SINR-driven TAS for $s_r=1$. It is quiet important to note that the terms that decay slowly in the summations in (70) are the second ones, i.e., $\dot{A}_2$ in $op^2_{s,snr}$ and $\ddot{A}_2$ in $op^2_{s,sinr}$, which justifies their appearance in (71). As for the achievable coding gains c^2_{snr} and c^2_{sinr}, they are given by

$$c^2_{snr}=\left[\frac{s_tr_es_r^2}{\lambda_{ss}^{s_rs_t}\lambda_{rs}^{s_rr_e}\,(s_r!)^{s_t+r_e}}\sum_{i=0}^{+\infty}\frac{1}{i!^2}\int_0^{+\infty}\int_0^{+\infty}\frac{q_1^{s_rs_t+i-1}q_2^{s_rr_e}}{(q_1+q_2)^{i+1}}\right.$$
$$\times\,\Gamma\left(1+i,\frac{(q_1+q_2)}{q_2}\frac{(q_1+\delta q_2)}{\alpha}\right)$$
$$\left.\times\;\Gamma\left(1+i,\frac{(q_1+q_2)}{q_2}\frac{q_1}{\alpha}\right)dq_2dq_1\right]^{-\frac{1}{s_r(s_t+r_e)}}\tag{72}$$

and

$$c^2_{sinr}=\left[\frac{s_t}{\lambda_{ss}^{s_t}\lambda_{rs}^{r_e}}\int_0^{+\infty}\int_0^{\alpha z}x^{s_t-1}e^{-z}\int_0^{+\infty}e^{-v}\right.$$
$$\times\left[\int_0^{+\infty}\mathcal{G}\left(\frac{(x+\delta x_2)(x+x_2)-\alpha\,(xz+x_2v)}{2\alpha\sqrt{zvxx_2}}\right)dx_2\right]^{r_e}$$
$$\left.\times\;dvdxdz\right]^{-\frac{1}{(s_t+r_e)}}\tag{73}$$

for $s_r=1$, respectively. The double integral in (72) can further be developed using [35, Eq. 8.352.2] as is the case for $\mathcal{I}_{\mathcal{R}_3}$ in (58). The function $\mathcal{G}(.)$ in (73) is already given by (69). Finally, we deduce from the asymptotic outage analysis of the end-to-end transmission of our incremental cognitive MIMO DF relay system the following remarks:

- Both TAS strategies under investigation achieve the same generalized diversity gain yet the SINR-driven TAS strategy has the advantage of achieving a better coding gain than the SNR-driven TAS strategy.
- Incremental cognitive MIMO DF relaying plays an important role in the enhancement of the achievable system diversity gain. In particular, s_t and r_e play interchangeable roles. This implies that whenever S-Tx can not support multiple antennas, Re is a good substitute in guaranteeing the same diversity gain.
- Since the second-order statistic λ_{ps} of the channel between P-Tx and S-Rx has a crucial impact on the overall system outage performance, it is highly recommended to adopt scheduling algorithms where S-Rx is selected on the basis of low λ_{ps} values.

VI. SIMULATION RESULTS AND IMPLEMENTATION PROSPECTS OF BOTH TAS/MRC STRATEGIES[5]

In this section, we confirm the correctness of the outage probability analysis carried out in the previous two sections, and importantly, compare between the SNR and SINR-driven TAS strategies proposed in the context of an incremental cognitive MIMO relaying setup. We give more insights on

[5]Throughout this section, the derived expressions involving infinite series are all convergent and truncated to $N\le200$ terms to achieve a relatively low truncation error ϵ [40] in the order of 10^{-3}.

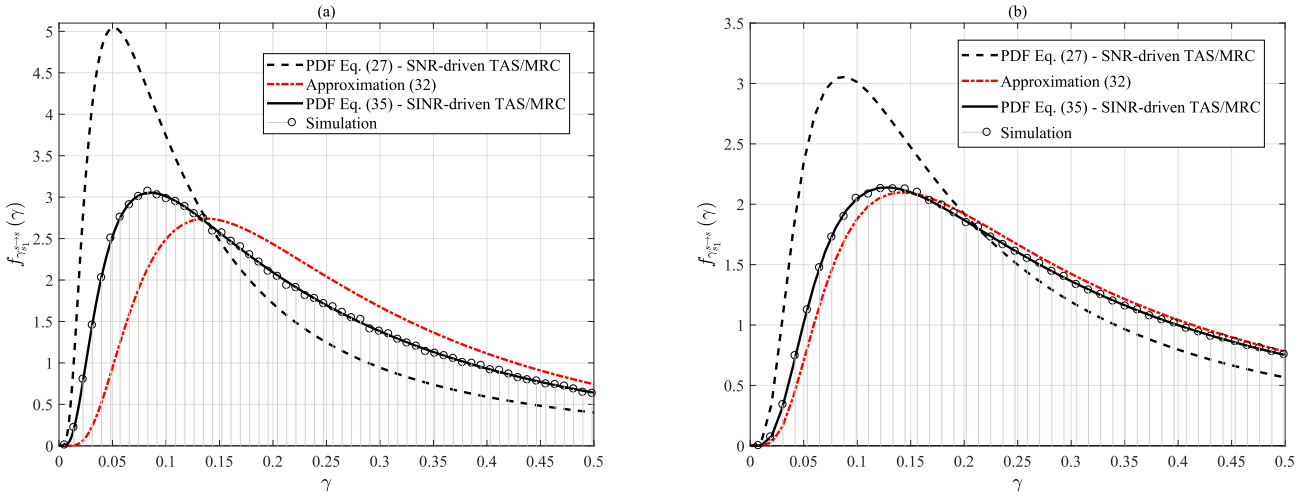

FIGURE 1. The MRC combiner output SINR PDFs (27) and (35) when the SNR and SINR-driven TAS/MRC strategies are adopted, respectively. Both PDFs are compared against the one generated according to approximation (32). For both figures, we have taken $\lambda_{ss} = \lambda_{sp} = \lambda_{ps} = 1$, $P_p/N_0 = 10$dB and $Q_i = -5$dB as practical system settings that can arbitrary be modified. The figure on the left (a) is generated for $s_t = 5$ and $s_r = 2$, whereas the figure on the right (b) is generated for $s_t = 2$ and $s_r = 5$. The index s_1 in $f_{\gamma_{s_1}^{s\to s}}(\gamma)$ equals either $\dot{s}_1$ or $\ddot{s}_1$ depending on the TAS/MRC strategy being utilized.

our results and discuss the implementation prospects of both TAS strategies under investigation.

A. PDF OF THE DIRECT-TRANSMISSION RECEIVED SINR AT S-Rx AND SOME INSIGHTS ON APPROXIMATION (32)

Fig. 1 shows the curves of the derived PDFs in (27) and (35) for both TAS strategies, thereby confirming the exactitude of our findings in subsection IV. As the receive antenna number s_r increases, as illustrated in Fig. 1-(b), the approximation (32) leading to

$$f_{\gamma_{\dot{s}_1}^{s\to s}}(\gamma) \approx s_t F_{\gamma_k^{s\to s}}(\gamma)^{s_t-1} f_{\gamma_k^{s\to s}}(\gamma) \tag{74}$$

becomes tight because the correlation between the received SINRs after MRC $\gamma_k^{s\to s}$ weakens. The evidence of this claim is justified by evaluating the correlation coefficient ζ^2 between the variables Z_k^1 in (31) that is found to be inversely proportional to s_r and exactly equaling $\zeta^2 = 1/s_r$. Hence, a typical scenario for which (74) holds as a tight approximation arises if a large-scale receive antenna array is deployed at S-Rx. This reasoning is valid only for the direct transmission, otherwise, (74) may not be adequate to approximate the PDF of the equivalent received SINR during the second relaying hop as the correlation between the resulting system variables become much more involved. From Fig. 2, we point out that the PDFs corresponding to both TAS strategies tend to approach each other for low values of λ_{ps}, and got clearly separated for high values of λ_{ps} reflecting the dominance of the interference from P-Tx on S-Rx. If the primary system interference on the secondary system is neglected, i.e., $\lambda_{ps} \to 0$, the SINR-driven TAS strategy reduces to its SNR-driven counterpart. Therefore, the former is viewed as an optimal interference-aware strategy that outperforms the latter over the entire primary system SNR ratio and for any arbitrary secondary system settings.

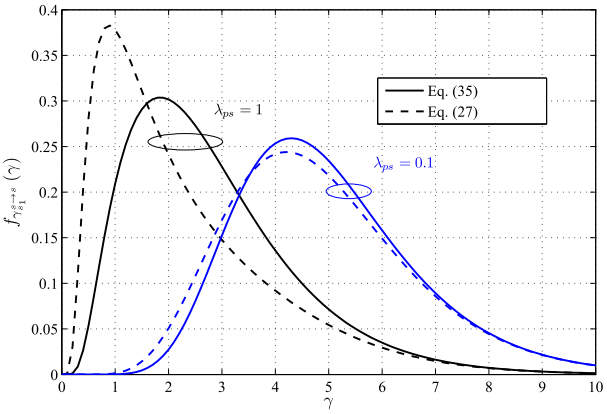

FIGURE 2. Comparison between the received SINR PDFs when an SNR and SINR-driven TAS strategies are adopted. It is assumed that $\lambda_{ss} = \lambda_{sp} = 1$, $P_p/N_0 = 5$dB, $Q_i = 0$dB and s_1 in $f_{\gamma_{s_1}^{s\to s}}(\gamma)$ equals either $\dot{s}_1$ or $\ddot{s}_1$ depending on the TAS strategy being utilized.

B. DIRECT-TRANSMISSION OUTAGE PROBABILITY

In Fig. 3-(a), the analytical expressions of the direct-transmission outage probability for both TAS schemes are depicted and compared to those found by Monte Carlo simulations, whereas in Fig. 3-(b), we separately plot the outage probability floor gap between both TAS strategies, $\triangle = opF^1_{s,sinr}/opF^1_{s,snr}$. Our curves are generated for different antenna configurations. Once again, our findings are confirmed by simulations to be exact and accurate. Pertaining to Fig. 3-(a), the secondary system transmit power P_s is allocated either in a fixed or adaptive manner as described in subsection II-B. Apparently, the former leads to severe performance degradation as opposed to the latter leading to a proportional outage performance enhancement with the primary system QoS. In the adaptive power allocation scenario, the

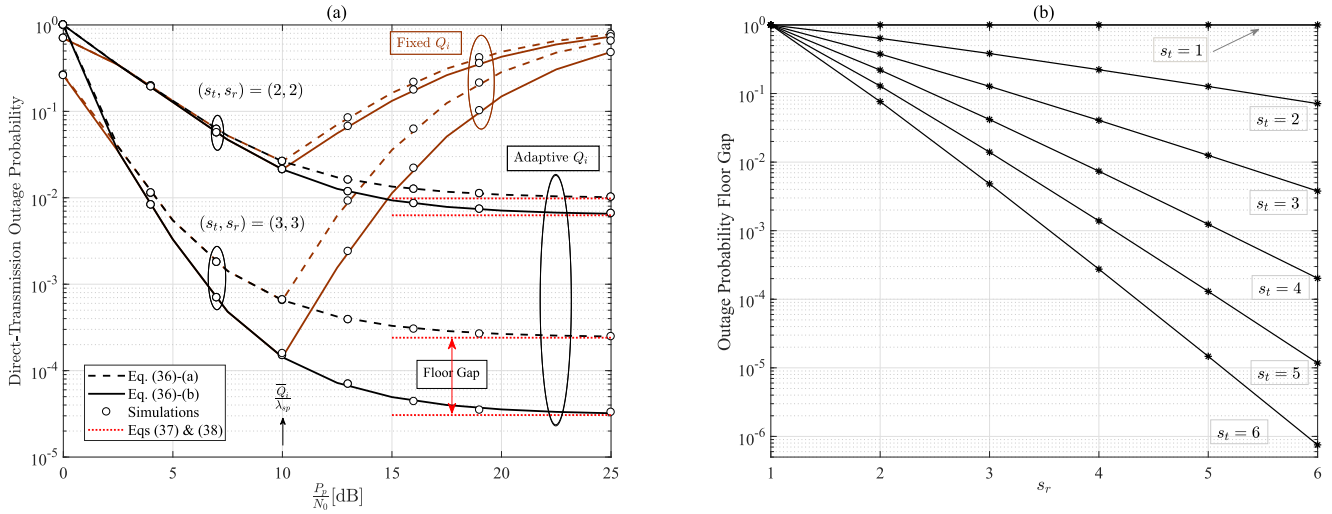

FIGURE 3. **(a): The direct-transmission outage probability $op^1_{s,snr}$ and $op^1_{s,sinr}$ at a certain threshold $\Phi_s = 2^2 - 1$ versus the primary system SNR ratio P_p/N_0 while having $\lambda_{ss} = 1$, $\lambda_{sp} = \lambda_{ps} = 0.1$ and $\overline{Q}_i = 0$dB fixed. (b): The outage probability floor gap between (37) and (38), appearing when $P_p/N_0 \to +\infty$, is calculated for different antenna configurations.**

condition $Q_i > 0$ according to (4) must hold or equivalently the primary system SNR ratio P_p/N_0 is required to be greater than a certain threshold Q_{th}dB, i.e.,

$$\frac{P_p}{N_0} > \frac{\Phi_p}{\lambda_{pp} \log\left(\frac{1}{1-\varepsilon_p}\right)} = 10^{\frac{Q_{th}}{10}},$$

so as the secondary system can coexist with the primary system on the same spectrum. Our simulations in Fig. (3) are conducted with $Q_{th} = -0.1$dB in order for the x-axis to be defined starting from $P_p/N_0 = 0$dB, and $\varepsilon_p = 0.01$. The value of Q_{th} can arbitrary be modified as a function of the primary system settings Φ_p, λ_{pp} and ε_p.

1) IMPACT OF ANTENNA CONFIGURATION

Fig 3-(b) shows the gap between both TAS strategies in terms of the ratio between (38) and (37) for different antenna configurations in the case of an adaptive power allocation is used by S-Tx. Clearly, the superiority of the SINR-driven TAS gets more pronounced for large-scale MIMO systems reflecting its co-channel interference cancellation capability compared to its SNR-driven counterpart. For instance, the outage probability floor gap for a 6×6 cognitive MIMO system is $\triangle = opF^1_{s,sinr}/opF^1_{s,snr} = (1.0784/1.43251) \times 10^{-6}$. We mention that this gap is attained in the high primary system SNR regime although the beginning of its appearance starts from low values of P_p/N_0 as captured by Fig. 3-(a).

2) IMPACT OF THE SECOND-ORDER STATISTIC λ_{ps}

Fig. 4 depicts the outage probability floors $opF^1_{s,snr}$ and $opF^1_{s,sinr}$ but now as a function of $1/\lambda_{ps}$. When large-scale variations of the interference channel between P-Tx and S-Rx are taken into account, λ_{ps} can be viewed as inversely proportional to the distance between P-Tx and S-Rx. This means that the greater $1/\lambda_{ps}$ is the farther P-Tx is seen from S-Rx. Therefore, the outage probability floors $opF^1_{s,snr}$ and $opF^1_{s,sinr}$ decrease as P-Tx goes far from S-Rx causing less interference on the secondary system. The gap between both TAS strategies widens for loaded cognitive MIMO configurations as the SINR-driven TAS strategy leverages all available cognitive MIMO system diversities to optimally reducing the primary system interference impact on the secondary system. Note that the general nature of our derived analytical framework serves to evaluate the secondary system outage performance under different system settings and scenarios for both TAS strategies.

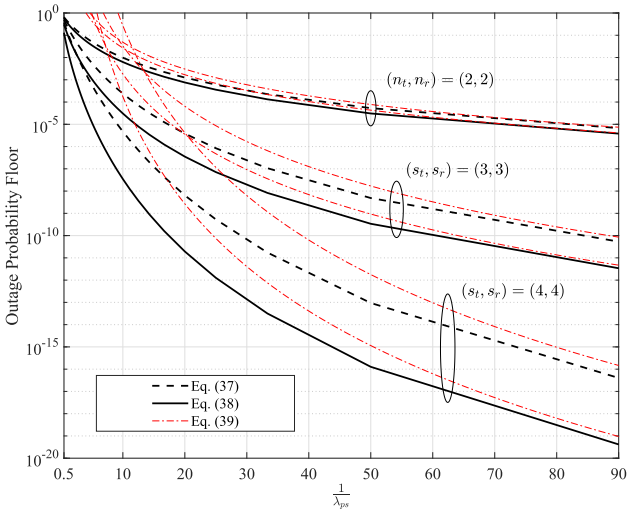

FIGURE 4. **The direct-transmission outage probability floor for both TAS strategies versus the inverse of λ_{ps} for different antenna configurations while $\lambda_{ss} = 1$, $\lambda_{sp} = 0.1$, $Q_{th} = -0.1$dB and $\varepsilon_p = 0.01$ are fixed.**

C. END-TO-END TRANSMISSION OUTAGE PERFORMANCE

During the second relaying hop, our cognitive $s_t \times s_r$ MIMO relay system can be viewed as a virtual cognitive $s_t \times 2s_r$ MIMO system thereby most of the insights provided in the

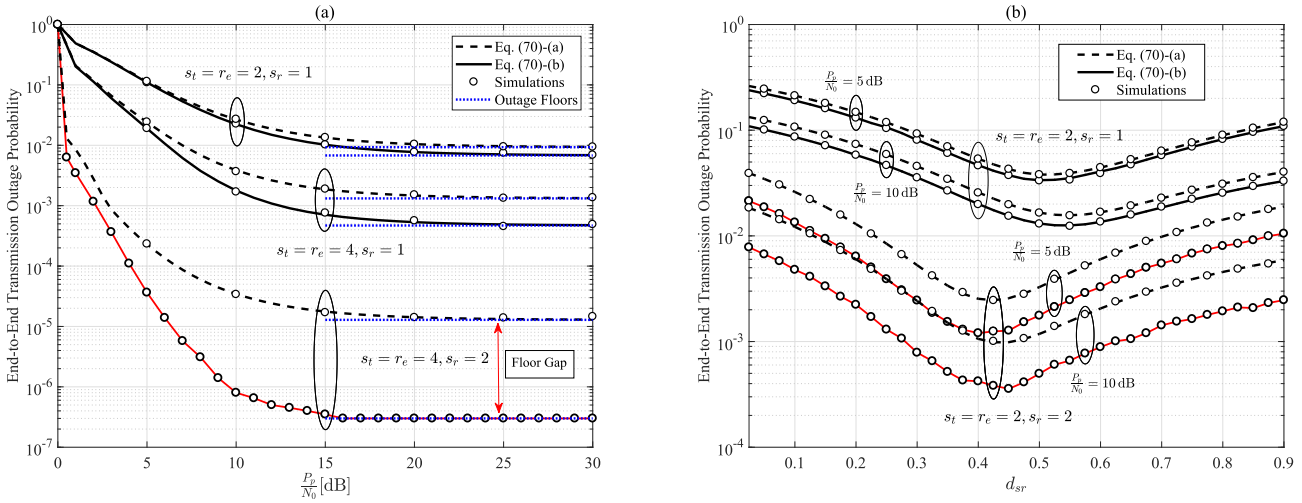

FIGURE 5. (a): Comparison of the derived end-to-end outage probability (70) for both TAS strategies under different MIMO relay system configurations while the parameters $\lambda_{ss} = 1$, $\lambda_{sr} = \lambda_{rs} = 0.4$, $\lambda_{sp} = \lambda_{ps} = 0.1$, $\lambda_{pr} = 0.6$, $\lambda_{rp} = 0.5$, $\Phi_s = 2^2 - 1$, $\varepsilon_p = 0.01$ and $Q_{th} = -0.1$dB are being fixed as exemplary parameters. (b): The end-to-end outage probability (70) versus d_{sr} for both TAS/MRC strategies.

previous subsection hold true herein as well. However, we are now much more interested in assessing the end-to-end outage performance of our system, in particular, the advantage of relaying and transmit diversities that are jointly targeted in the proposed SINR-driven TAS strategy.

1) IMPACT OF ANTENNA CONFIGURATION

In Fig. 5-(a), our derived analytical results of the end-to-end transmission outage probability (70) for both TAS strategies under focus are compared and validated by simulations. Note that the curves representing the SINR-driven TAS/MRC in the case of $s_r = 1$ corresponds to the end-to-end transmission outage analysis carried out in subsections V-C, V-A and V-D. As already pointed out, for situations where $s_r \geq 2$, the end-to-end outage probability when an SINR-driven TAS/MRC strategy is adopted becomes too complex to evaluate analytically, therefore, we resort to Monte Carlo simulations as depicted in red solid lines in Fig. 5.

2) IMPACT OF RELAY LOCATION

Fig. 5-(b) shows the end-to-end outage probability as a function of the distance between S-Tx and Re. For simplicity, we consider a two-dimensional squared geometry [11] of our cognitive MIMO relay system where P-Tx, P-Rx, S-Tx and S-Rx are positioned at locations of coordinates (1,0), (1,1), (0,0), (0,1), respectively, and Re moves across the line between S-Tx and S-Rx. Our path-loss model is assumed to be exponentially decaying such that $\lambda_{ab} = d_{ab}^{-\kappa}$ where d_{ab} is the distance between the transmitting node of index a and the receiving node of index b, and κ is the path-loss coefficient. From Fig 5(b), we observe that the optimal relay location is centered around $d_{sr} = 0.5$, but tends to shrink as s_r increases and enlarges as s_r decreases. This is true whether the secondary system is operating at low or moderate-to-high primary system SNR ratios.

D. IMPLEMENTATION PROSPECTS OF BOTH TAS/MRC STRATEGIES

1) ANTENNA INDEX FEEDBACK LOAD

During both relaying hops, the secondary system transmitting nodes need to identify the index of their transmit antenna. This index is assumed to be selected by S-Rx but fed back to either S-Tx or Re via an error-free load of $\max\left\{\lceil \log_2(s_t) \rceil, \lceil \log_2(r_e) \rceil\right\}$ binary bits where $\lceil u \rceil$ refers to the smallest integer greater than or equals u. In this regard, both TAS strategies are alike.

2) CSI ACQUISITION AND ANTENNA SELECTION

Assuming the secondary system receiving node S-Rx is capable of acquiring complete CSI about the links $\{s \to s\}$ and $\{r \to s\}$, it can simply identify the index of the transmit antenna at either S-Tx or Re according to the SNR-driven TAS strategy. Yet, for symbol decoding purposes, S-Rx is required to also acquire complete CSI about the interference link $\{p \to s\}$ and determine the primary and secondary transmit power levels in addition to the AWGN power spectral density. Altogether, these parameters are the prerequisites of the SINR-driven TAS strategy. Hence, while the SNR-driven TAS strategy can be applied at an early stage of the symbol decoding process at S-Rx, its SINR-driven counterpart requires additional parameters that are needed anyway in the decoding process at S-Rx. This justifies the performance/complexity tradeoff by which both TAS strategies are governed.

3) TAS IN BEYOND 5G WIRELESS COMMUNICATIONS

In LTE, the concept of TAS was used as a cost-effective means to reduce system complexity and power consumption at the user equipment side while reaping the benefits of multi-antenna systems. Among other advantages, its flexibility and adaptability [33] to be coupled with different MIMO variants

such as spatial-division multiplexing and space-time block codes makes it a potential technology candidate for future wireless networks. Importantly, TAS can also be envisaged for massive MIMO systems along with spatial and index modulations to mitigate co-channel interference in a more sophisticated way [34]. In beyond 5G wireless networks, the sources of interference are diverse and sometimes controlled as is the case in the cognitive underlay paradigm. Therefore, in order to leverage the antenna selection benefits, particular efforts should be paid to the joint design of efficient antenna selection algorithms at the transmitter and receiver sides.

VII. CONCLUSION

We have conducted an exact and asymptotic outage performance analysis of incremental cognitive MIMO DF relaying systems for two TAS strategies that are driven by maximizing either the received SNR or SINR ratios. For each relaying hop and each TAS strategy, we thoroughly analyzed the statistics of the received SINR and derived new results in terms of the direct and end-to-end transmission outage performance. Finally, our analytical and simulation results are evaluated while revealing the accuracy of our developments and optimality of the SINR-driven TAS strategy.

APPENDIX

A. PROOF OF PROPOSITION 1

To resolve (2), it suffices to derive the primary system outage probability op_p. Since P-Tx and P-Rx are equipped with a single antenna, the primary system falls in outage if the received SINR at P-Rx (at each relaying hop) is less than a certain threshold Φ_p, i.e.,

$$op_p = \mathcal{P}\left(\frac{P_p X}{PZ + N_0} < \Phi_p\right), \tag{75}$$

where $X = \left|h_{1,1}^{p\to p}\right|^2$ and $Z = \left|h_{1,k}^{s\to p}\right|^2$ are the power gains of the channel links $\{p \to p\}$ and $\{s \to p\}$, respectively. Kindly note that X and Z are independent yet not identically distributed Exponential random variables with parameters λ_{pp} and λ_{sp}, respectively. The index k in $h_{1,k}^{s\to p}$ refers to the transmit antenna selected by S-Tx. Using the total probability law through conditioning on Z, (75) can be rewritten as

$$op_p = \int_0^{+\infty} \underbrace{\mathcal{P}\left(X < \frac{\Phi_p}{P_p}(Pz + N_0)\right)}_{=F_X\left(\frac{\Phi_p}{P_p}(Pz+N_0)\right)} f_Z(z)\, dz, \tag{76}$$

where $f_Z(z) = \left(e^{-\frac{z}{\lambda_{sp}}}/\lambda_{sp}\right) U(z)$ and $F_X(x) = \left(1 - e^{-\frac{x}{\lambda_{pp}}}\right) U(x)$ whereas $U(.)$ is the unit step function. Substituting the latter functions into (76), we obtain via simple integral manipulations

$$op_p = \int_0^{+\infty} \left(1 - e^{-\frac{\Phi_p(Pz+N_0)}{P_p\lambda_{pp}}}\right) \frac{e^{-\frac{z}{\lambda_{sp}}}}{\lambda_{sp}} dz \tag{77}$$

$$= 1 - e^{-\frac{\Phi_p N_0}{P_p\lambda_{pp}}} \left(\frac{\Phi_p P \lambda_{sp}}{P_p \lambda_{pp}} + 1\right)^{-1}. \tag{78}$$

It follows then that the solution P to (2) is given by (3).

B. DERIVATION OF EQ. (24)

By treating $\overline{\gamma}(l,x)^k$ as a binomial, we get

$$\overline{\gamma}(l,x)^k = \sum_{i_1=0}^{k} \binom{k}{i_1} (-1)^{i_1} e^{-x} \left(\sum_{i=0}^{l-1} \frac{x^i}{i!}\right)^{i_1} \tag{79}$$

$$= \sum_{i_1=0}^{k} \binom{k}{i_1} (-1)^{i_1} e^{-x} \sum_{i_2=0}^{i_1(l-1)} \varphi_{i_1,i_2}^{k,l} x^{i_2}, \tag{80}$$

where, in (80), we explored the fact that the above $(l-1)$-degree polynomial to the power of i_1 is also a polynomial whose degree is $i_1(l-1)$. The resulting polynomial coefficients are given by

$$\varphi_{i_1,i_2}^{k,l} = \frac{1}{i_2!} \mathcal{D}_x \left[\left(\sum_{i=0}^{l-1} \frac{x^i}{i!}\right)^{i_1}\right]^{(i_2)}\Bigg|_{x=0}. \tag{81}$$

In (81), $\mathcal{D}_x[.]^{(i_2)}$ denotes the i_2th order derivative operator with respect to x. Hence, (81) can alternatively be expressed with the help of [35, 0.314] for $i_1 \in \{0,\ldots,k\}$ and $i_2 \in \{0,\ldots,i_1(l-1)\}$ in the form of the following recursion

$$\begin{cases} \varphi_{i_1,0}^{k,l} = 1, & i_2 = 0 \\ \varphi_{i_1,i_2}^{k,l} = \dfrac{1}{i_2} \displaystyle\sum_{i_3=1}^{\min(i_2,l-1)} \frac{(i_3 i_1 - i_2 + i_3)}{i_3!} \varphi_{i_1,i_2-i_3}^{k,l}, & 1 \le i_2 \end{cases} \tag{82}$$

resulting in (24) where $\psi_{i_1,i_2}^{k,l} = \binom{k}{i_1}(-1)^{i_1} \varphi_{i_1,i_2}^{k,l}$.

C. PROOF OF THEOREM 1

To accurately derive (28), we rewrite the variable Z_k^1 in (31) as

$$Z_k^1 = \frac{\left|\boldsymbol{h}_k^{1,s\to s^H} \boldsymbol{h}_1^{1,p\to s}\right|^2}{\left\|\boldsymbol{h}_k^{1,s\to s}\right\|^2} = \frac{Y_k^1}{X_k^1} V, \tag{83}$$

where $Y_k^1 = \left|\boldsymbol{h}_k^{1,s\to s^H} \boldsymbol{h}_1^{1,p\to s}\right|^2 / V$, $V = \left\|\boldsymbol{h}_1^{1,p\to s}\right\|^2$ and $X_k^1 = \left\|\boldsymbol{h}_k^{1,s\to s}\right\|^2$. Note that X_k^1 and the newly introduced variable Y_k^1 are still dependent variables following Gamma and Exponential distributions, respectively. However, to get rid of the maximum operator in (29) after being plug into (28), it suffices to condition the variable Z_k^1 on V because the latter appears to be the cause of dependence between the received

SINRs, $\gamma_k^{s\to s} = P_s X_k^1 / \left(P_p Z_k^1 + N_0\right)$ for $k \in \{1, \ldots, s_t\}$. Hence, (28) can now precisely be expressed as

$$F_{\gamma_{s_1}^{s\to s}}(\gamma) = \int_0^{+\infty} \mathcal{P}\left(\frac{P_s X_k^1}{P_p \frac{Y_k^1}{X_k^1} v + N_0} < \gamma\right)^{s_t} f_V(v)\, dv, \quad (84)$$

where the PDF of the Gamma variable V is given by

$$f_V(v) = \frac{v^{s_r-1} e^{-\frac{v}{\lambda_{ps}}}}{\lambda_{ps}^{s_r}\Gamma(s_r)} U(v). \quad (85)$$

The difference between (30) and (84) lies in the exponent s_t that is now correctly appearing inside the integral.

Because the following quadratic inequality

$$\frac{\boldsymbol{h}_1^{1,p\to s^H} \boldsymbol{h}_k^{1,s\to s} \boldsymbol{h}_k^{1,s\to s^H} \boldsymbol{h}_1^{1,p\to s}}{\left\|\boldsymbol{h}^{1,p\to s}\right\|^2} \le \left\|\boldsymbol{h}_k^{1,s\to s}\right\|^2 \quad (86)$$

holds true in general for any arbitrary channel vectors $\boldsymbol{h}_k^{1,s\to s}$ and $\boldsymbol{h}_1^{1,p\to s} \neq \boldsymbol{0}$, it can be proved that the joint PDF of X_k^1 and $Y_k^1|v$, $f_{X_k^1, Y_k^1|v}(,)$ coincides with the McKay's bivariate Gamma distribution [38] given by

$$f_{X_k^1, Y_k^1|v}(x, y) = \frac{(x-y)^{s_r-2} e^{-\frac{x}{\lambda_{ss}}}}{\lambda_{ss}^{s_r}\Gamma(s_r-1)} U(x-y) \quad (87)$$

for a number of receive antennas $s_r \ge 2$. We deduce from (87) that X_k^1 and Y_k^1 are jointly independent from V. Hence, the probability inside (84), after carefully defining our integration regions, can be rewritten as

$$\begin{aligned}
&\mathcal{P}\left(\gamma_k^{s\to s} \middle| v < \gamma\right) \\
&= \underbrace{\int_0^{\frac{\gamma N_0}{P_s}} \int_0^{x} \frac{(x-y)^{s_r-2} e^{-\frac{x}{\lambda_{ss}}}}{\lambda_{ss}^{s_r}\Gamma(s_r-1)} dy dx}_{\mathcal{J}_1(\gamma)} \\
&\quad + \underbrace{\int_{\frac{\gamma N_0}{P_s}}^{\frac{\gamma}{P_s}(P_p v + N_0)} \int_{\frac{-\gamma N_0 x + P_s x^2}{\gamma P_p v}}^{x} \frac{(x-y)^{s_r-2} e^{-\frac{x}{\lambda_{ss}}}}{\lambda_{ss}^{s_r}\Gamma(s_r-1)} dy dx}_{\mathcal{J}_2(\gamma, v)}. \quad (88)
\end{aligned}$$

It can be shown with the help of [35, 3.351.1] that the first term $\mathcal{J}_1(\gamma)$ of the right-hand side of (88) is the regularized lower incomplete Gamma function,

$$\mathcal{J}_1(\gamma) = \overline{\gamma}\left(s_r, \frac{\gamma N_0}{P_s \lambda_{ss}}\right), \quad (89)$$

while the first integral in the second term $\mathcal{J}_2(\gamma, v)$ can further be developed as

$$\begin{aligned}
\mathcal{J}_2(\gamma, v) = &\int_{\frac{\gamma N_0}{P_s}}^{\frac{\gamma}{P_s}(P_p v + N_0)} \frac{x^{s_r-1} e^{-\frac{x}{\lambda_{ss}}}}{\Gamma(s_r)} \\
&\times \left(\frac{P_s}{\gamma P_p v}\left(\frac{\gamma}{P_s}\left(P_p v + N_0\right) - x\right)\right)^{s_r-1} dx. \quad (90)
\end{aligned}$$

After making the change of variable $t = \frac{\gamma}{P_s}\left(P_p v + N_0\right) - x$, (90) can be evaluated by expanding the resulting binomial inside the integral and using [35, 3.351.1] as

$$\begin{aligned}
\mathcal{J}_2(\gamma, v) = &\frac{(-1)^{s_r} e^{-\frac{\gamma N_0}{P_s \lambda_{ss}}}}{\Gamma(s_r)} \sum_{k=0}^{s_r-1} \binom{s_r-1}{k} \left(\frac{P_s \lambda_{ss}}{\gamma}\right)^k \\
&\times e^{-\frac{\gamma P_p v}{P_s \lambda_{ss}}} \frac{\left(P_p v + N_0\right)^{s_r-1-k}}{\left(P_p v\right)^{s_r-1}} \gamma\left(s_r + k, -\frac{\gamma P_p v}{P_s \lambda_{ss}}\right). \quad (91)
\end{aligned}$$

Once we replace (89) and (91) into (88), raised to the power of s_t, the result can be treated as a binomial whose expansion can be expressed as

$$\begin{aligned}
&\mathcal{P}\left(\gamma_k^{s\to s} \middle| v < \gamma\right)^{s_t} \\
&= \overline{\gamma}\left(n_r, \frac{\gamma N_0}{P_s \lambda_{ss}}\right)^{s_t} + \sum_{l=1}^{s_t} \binom{s_t}{l} \\
&\quad \times \overline{\gamma}\left(n_r, \frac{\gamma N_0}{P_s \lambda_{ss}}\right)^{s_t - l} \frac{(-1)^{l s_r} e^{-\frac{\gamma N_0 l}{P_s \lambda_{ss}}}}{\Gamma(s_r)^l} \left(\frac{P_s \lambda_{ss}}{\gamma}\right)^{\sum_{i=1}^l k_i} \\
&\quad \times \sum_{0 \le k_1, \ldots, k_l \le s_r - 1} \prod_{i=1}^{l} \binom{s_r - 1}{k_i} \left(P_p v\right)^{l(s_r-1)} \\
&\quad \times \left(P_p v + N_0\right)^{l(s_r-1) - \sum_{i=1}^l k_i} e^{-\frac{\gamma P_p v l}{P_s \lambda_{ss}}} \\
&\quad \times \prod_{i=1}^{l} \gamma\left(s_r + k_i, \frac{-\gamma P_p v}{P_s \lambda_{ss}}\right), \quad (92)
\end{aligned}$$

where we pulled out to the right the terms containing the variable v. Prior to carrying the integration over v as in (84), the product of the lower incomplete Gamma functions in the last line of (92) is evaluated with the help of [35, 8.354.1] as

$$\begin{aligned}
&\prod_{i=1}^{l} \gamma\left(s_r + k_i, \frac{-\gamma P_p v}{P_s \lambda_{ss}}\right) \\
&\quad = \sum_{n=0}^{+\infty} \mathcal{A}_{l,n}^{s_r}(k_1, \ldots, k_l) \left(-\frac{\gamma P_p v}{P_s \lambda_{ss}}\right)^{\sum_{i=1}^l k_i + l s_r + n}, \quad (93)
\end{aligned}$$

where the coefficients $\mathcal{A}_{l,n}^{s_r}(., \ldots, .)$ for an integer $n \ge 0$ are given by (34). Finally, by replacing (93) into (92), we obtain an exact expression of the CDF of $\gamma_{s_1}^{s\to s}$ as in (33). Note that the infinite summation in (93) might be avoided if we use the approach presented in [36, Eq. 13] thereby the product of the lower incomplete Gamma functions can be expressed in closed form. However, the featured property of the infinite summation lies in its exponent beginning from $k_i + s_r$ (for $n = 0$) for each function $\gamma\left(s_r + k_i, -\gamma P_p v / P_s \lambda_{ss}\right)$ where i ranges from 1 to l. That is, the product (93) results in a polynomial whose first-term exponent is $\sum_{i=1}^l k_i + l s_r$ that, once replaced into (92), reduces with $-\sum_{i=1}^l k_i$. As an important consequence, (92) does not present any non-integrable singularity points.

D. PROOF OF COROLLARY 1

To proceed with the PDF derivation of the received SINR, $\gamma_{\dot{s}_1}^{s\to s}$, it follows from (84) that

$$f_{\gamma_{\dot{s}_1}^{s\to s}}(\gamma) = s_t \int_0^{+\infty} \mathcal{P}\left(\gamma_k^{s\to s}\middle| v<\gamma\right)^{s_t-1} \times \left(\mathcal{DJ}_1(\gamma)+\mathcal{DJ}_2(\gamma,v)\right) f_V(v)\,dv, \quad (94)$$

where $\mathcal{DJ}_1$ is evaluated as

$$\mathcal{DJ}_1 = \frac{\partial}{\partial\gamma}\overline{\gamma}\left(s_r, \frac{\gamma N_0}{P_s\lambda_{ss}}\right) = \frac{\gamma^{s_r-1}e^{-\frac{\gamma N_0}{P_s\lambda_{ss}}}}{\left(\frac{P_s\lambda_{ss}}{N_0}\right)^{s_r}\Gamma(s_r)} \quad (95)$$

and

$$\mathcal{DJ}_2(\gamma,v) = \frac{\partial}{\partial\gamma}\int_{\frac{\gamma N_0}{P_s}}^{\frac{\gamma}{P_s}(P_pv+N_0)} \frac{x^{s_r-1}e^{-\frac{x}{\lambda_{ss}}}}{\lambda_{ss}^{s_r}\Gamma(s_r)} \times\left(\frac{P_s}{\gamma P_pv}\left(\frac{\gamma}{P_s}\left(P_pv+N_0\right)-x\right)\right)^{s_r-1}dx. \quad (96)$$

Using the general Leibniz rule for partial derivative of integrals and identical steps used to derive $\mathcal{J}_2(v)$ (91), $\mathcal{DJ}_2(v)$ can be expressed as

$$\mathcal{DJ}_2(\gamma,v) = -\frac{\gamma^{s_r-1}e^{-\frac{\gamma N_0}{P_s\lambda_{ss}}}}{\left(\frac{P_s\lambda_{ss}}{N_0}\right)^{s_r}\Gamma(s_r)} + \frac{(-1)^{s_r-1}e^{-\frac{\gamma N_0}{\lambda_{ss}P_s}}}{\lambda_{ss}\Gamma(s_r-1)P_s} \times\sum_{k=0}^{s_r}\binom{s_r}{k}\left(\frac{P_s\lambda_{ss}}{\gamma}\right)^k e^{-\frac{\gamma P_pv}{\lambda_{ss}P_s}}\frac{\left(P_pv+N_0\right)^{s_r-k}}{\left(P_pv\right)^{s_r-1}} \times\gamma\left(s_r+k-1,-\frac{P_pv\gamma}{P_s\lambda_{ss}}\right). \quad (97)$$

Adding $\mathcal{DJ}_2(\gamma,v)$ to $\mathcal{DJ}_1(v)$ and replacing the result into (94), it follows from applying the same approach used to derive $F_{\gamma_{\dot{s}_1}^{s\to s}}(.)$ that the PDF of $\gamma_{\dot{s}_1}^{s\to s}$ is given by (35).

E. PROOF OF EQUATIONS (37), (38) AND (39)

As $P_p/N_0\to+\infty$, we obtain from (23),

$$opF_{s,snr}^1 = \int_0^{+\infty}\overline{\gamma}\left(s_r,\frac{\Phi_sz}{\eta\lambda_{ss}}\right)^{s_t}\frac{e^{-\frac{z}{\lambda_{ps}}}}{\lambda_{ps}}dz, \quad (98)$$

where $\eta=\lim_{\frac{P_p}{N_0}\to+\infty}\frac{P_s}{P_p}$ is given by (40). (98) is evaluated using Lemma 1 as in (37). To derive the asymptotic expression of $opF_{s,snr}^1$ for $\lambda_{ps}\to0$, we make the change of variable $t=\frac{z}{\lambda_{ps}}$ inside the integral in (98). The resulting expression is given by

$$opF_{s,snr}^1 = \int_0^{+\infty}\overline{\gamma}\left(s_r,\frac{\Phi_s\lambda_{ps}t}{\eta\lambda_{ss}}\right)^{s_t}e^{-t}dz \underset{\lambda_{ps}\to0}{\approx} \frac{\left(\frac{\Phi_s\lambda_{ps}}{\eta\lambda_{ss}}\right)^{s_rs_t}}{(s_r!)^{s_t}}\int_0^{+\infty}t^{s_rs_t}e^{-t}dt, \quad (99)$$

where we exploited the fact that $\overline{\gamma}(n,\lambda)\approx\lambda^n/n!$ as $\lambda\to0$ for an integer n and real λ. Using [35, Eq. 3.351.3], (99) can be expressed as (37). Pertaining to the SINR-driven TAS/MRC strategy, (84) converges as $\lambda_{ps}\to0$ to

$$opF_{s,sinr}^1 = \int_0^{+\infty}\mathcal{P}\left(\eta X_k^{1^2}<\Phi_sY_k^1v\right)^{s_t}\frac{v^{s_r-1}e^{-\frac{v}{\lambda_{ps}}}}{\lambda_{ps}^{s_r}\Gamma(s_r)}dv. \quad (100)$$

Similar to the approach used to derive $op_{s,sinr}^1$, the probability inside the integral in (100) now reduces from (88) to

$$\mathcal{P}\left(\eta X_k^{1^2}<\Phi_sY_k^1v\right) = \frac{(-1)^{s_r}e^{-\frac{\Phi_sv}{\eta\lambda_{ss}}}}{\Gamma(s_r)}\sum_{k=0}^{s_r-1}\binom{s_r-1}{k} \times\left(\frac{\eta\lambda_{ss}}{\Phi_sv}\right)^k\gamma\left(s_r+k,-\frac{\Phi_sv}{\eta\lambda_{ss}}\right), \quad (101)$$

raised to the power of s_t then substituted into (100), we finally obtain an exact expression of $opF_{s,sinr}^1$ that is explicitly given by (38). Asymptotically, i.e., when $\lambda_{ps}\to0$, (101) converges after making the aforementioned change variable to

$$opA_{s,sinr}^1 = \frac{\left(\frac{\Phi_s\lambda_{ps}}{\eta\lambda_{ss}}\right)^{s_rs_t}}{\Gamma(s_r)^{s_t+1}}S^{s_t}\int_0^{+\infty}t^{s_rs_t+s_r-1}e^{-t}dt, \quad (102)$$

where the sum S is evaluated with the help of [35, Eq. 0.160.2] in terms of the Beta function [35, Eq. 8.380.1] as

$$S = \sum_{k=0}^{s_r-1}\binom{s_r-1}{k}\frac{(-1)^k}{(s_r+k)} = \mathcal{B}(s_r,s_r) = 2^{1-2s_r}\mathcal{B}\left(\frac{1}{2},s_r\right) = \frac{2^{1-2s_r}\sqrt{\pi}\Gamma(s_r)}{\Gamma\left(\frac{1}{2}+s_r\right)}. \quad (103)$$

The second line (103) follows from the use of [35, Eqs 8.384.4, 8.384.1, 8.338.2]. Therefore, using [35, Eq. 3.351.3], (102) can finally be rewritten as in the second line of (39).

F. DERIVATION OF ρ_x^2 AND ρ^2

By definition, we have

$$\rho^2 = \frac{E\left[Z_{\dot{s}_1}^1Z_{\dot{s}_1,\dot{r}}^2\right]-\lambda_{ps}^2}{\lambda_{ps}^2}, \quad (104)$$

where $Z_{\dot{s}_1}^1$ and $Z_{\dot{s}_1,\dot{r}}^2$ are to be replaced by (20) and (46), respectively, into (104). Then, by carrying the expectation $E\left[Z_{\dot{s}_1}^1Z_{\dot{s}_1,\dot{r}}^2\right]$ firstly over $\boldsymbol{h}_1^{2,p\to s}$, we get

$$E\left[Z_{\dot{s}_1}^1Z_{\dot{s}_1,\dot{r}}^2\right] = E\left(\frac{Z_{\dot{s}_1}^{1^2}X_{\dot{s}_1}^1}{X_{\dot{s}_1}^1+X_{\dot{r}}}+\frac{\lambda_{ps}Z_{\dot{s}_1}^1X_{\dot{r}}}{X_{\dot{s}_1}^1+X_{\dot{r}}}\right) \quad (105)$$

$$= \lambda_{ps}^2E\left(\frac{2X_{\dot{s}_1}^1+X_{\dot{r}}}{X_{\dot{s}_1}^1+X_{\dot{r}}}\right), \quad (106)$$

where the second line follows from carrying the expectation over $Z^1_{\dot{s}_1}$ (105) recalling that $Z^1_{\dot{s}_1}$ alone is independent of $X^1_{\dot{s}_1}$ and $X_{\dot{r}}$. Hence, we have

$$\rho_x^2 = \frac{x_1}{(x_1 + x_2)} \tag{107}$$

and

$$\rho^2 = E\left[\frac{X^1_{\dot{s}_1}}{X^1_{\dot{s}_1} + X_{\dot{r}}}\right] \tag{108}$$

$$= \int_0^{+\infty}\int_0^{+\infty} \frac{x_1}{x_1 + x_2} f_{X^1_{\dot{s}_1}}(x_1) f_{X_{\dot{r}}}(x_2)\, dx_1 dx_2, \tag{109}$$

where $f_{X^1_{\dot{s}_1}}(.)$ is given by (22) while $f_{X_{\dot{r}}}(.)$ is deduced from (22) by replacing s_t and λ_{ss} by r_e and λ_{rs}, respectively. To calculate ρ^2, we expand $f_{X^1_{\dot{s}_1}}(.)$ and $f_{X_{\dot{r}}}(.)$ using Lemma 1 before being substituted in (109). With the help of [37, Vol 1: Eq. 3.1.3.5], we end up with (51).

G. PROOF OF THEOREM 2

According to (63), $Z^2_{\dot{s}_1,k}|x, z, v$ expands for $s_r = 1$ as

$$Z^2_{\dot{s}_1,k}|x, z, v = xz + X_k v + 2\sqrt{xzX_k v}\cos(\Omega), \tag{110}$$

where Ω is a random variable that is Uniformally distributed over $[-\pi, \pi[$. Hence, the derivative of the CDF $F_{\cos(\Omega)}(w) = F_\Omega(\arccos(w))$ with respect to w results in

$$f_{\cos(\Omega)}(w) = \begin{cases} \dfrac{1}{\pi\sqrt{1-w^2}}; & -1 < w < 1 \\ 0; & \text{Otherwise.} \end{cases} \tag{111}$$

We deduce that $Z^2_{\dot{s}_1,k}|x, z, v$ conditioned on $X_k = x_2$ for $k \in \{1, \ldots, r_e\}$ is drawn from the following distribution

$$f_{Z^2_{\dot{s}_1,k}|x,z,v,x_2}(z_2) = \begin{cases} \dfrac{1}{\pi\sqrt{4xzx_2v - (z_2 - (xz + x_2v))^2}}; \\ \quad \left(\sqrt{xz} - \sqrt{x_2v}\right)^2 < z_2 < \left(\sqrt{xz} + \sqrt{x_2v}\right)^2 \\ 0; \quad \text{Otherwise.} \end{cases} \tag{112}$$

Since X_k is an Exponential random variable with parameter λ_{rs}, then by applying Bayes Theorem, we obtain (64) and conclude with the proof of Theorem 2.

REFERENCES

[1] P. Kolodzy, "Spectrum policy task force," Federal Commun. Commission, Washington, DC, USA, Tech. Rep. ET Docket 02-135, Nov. 2002.
[2] A. Goldsmith, S. A. Jafar, I. Maric, and S. Srinivasa, "Breaking spectrum gridlock with cognitive radios: An information theoretic perspective," *Proc. IEEE*, vol. 97, no. 5, pp. 894–914, May 2009.
[3] K. Huang and R. Zhang, "Cooperative feedback for multiantenna cognitive radio networks," *IEEE Trans. Signal Process.*, vol. 59, no. 2, pp. 747–758, Feb. 2011.
[4] J. Lui, W. Chen, Z. Cao, and Y. J. A. Zhang, "Cooperative beamforming for cognitive radio networks: A cross-layer design," *IEEE Trans. Wireless Commun.*, vol. 60, no. 5, pp. 1420–1431, May 2012.
[5] L. Sboui, H. Ghazzai, Z. Rezki, and M.-S. Alouini, "Precoder design and power allocation for MIMO cognitive radio two-way relaying systems," *IEEE Trans. Commun.*, vol. 64, no. 10, pp. 4111–4120, Oct. 2016.
[6] B.-J. Lee, S.-L. Ju, N.-I. Kim, and K.-S. Kim, "Enhanced transmit-antenna selection schemes for multiuser massive MIMO systems," *Wireless Commun. Mobile Comput.*, vol. 2017, Jun. 2017, Art. no. 3463950.
[7] Z. Chen, J. Yuan, and B. Vucetic, "Analysis of transmit antenna selection/maximal-ratio combining in Rayleigh fading channels," *IEEE Trans. Veh. Technol.*, vol. 54, no. 4, pp. 1312–1321, Jul. 2005.
[8] T. K. Y. Lo, "Maximum ratio transmission," *IEEE Trans. Commun.*, vol. 47, no. 10, pp. 1458–1461, Oct. 1999.
[9] Y. Chen and C. Tellambura, "Performance analysis of maximum ratio transmission with imperfect channel estimation," *IEEE Commun. Lett.*, vol. 9, no. 4, pp. 322–324, Apr. 2005.
[10] M. C. Ilter, P. A. Dmochowski, and H. Yanikomeroglu, "Revisiting error analysis in convolutionally coded systems: The irregular constellation case," *IEEE Trans. Commun.*, vol. 66, no. 2, pp. 465–477, Feb. 2018.
[11] P. L. Yeoh, M. Elkashlan, K. J. Kim, T. Q. Duong, and G. K. Karagiannidis, "Transmit antenna selection in cognitive MIMO relaying with multiple primary transceivers," *IEEE Trans. Veh. Technol.*, vol. 65, no. 1, pp. 483–489, Jan. 2016.
[12] P. L. Yeoh, M. Elkashlan, T. Q. Duong, N. Yang, and D. B. da Costa, "Transmit antenna selection for interference management in cognitive relay networks," *IEEE Trans. Veh. Technol.*, vol. 63, no. 7, pp. 3250–3262, Sep. 2014.
[13] F. S. Al-Qahtani, R. M. Radaydeh, S. Hessien, T. Q. Duong, and H. Alnuweiri, "Underlay cognitive multihop MIMO networks with and without receive interference cancellation," *IEEE Trans. Commun.*, vol. 65, no. 4, pp. 1477–1493, Apr. 2017.
[14] E. Erdogan, A. Afana, S. Ikki, and H. Yanikomeroglu, "Antenna selection in MIMO cognitive AF relay networks with mutual interference and limited feedback," *IEEE Commun. Lett.*, vol. 21, no. 5, pp. 1111–1114, May 2017.
[15] K. Tourki, F. A. Khan, K. A. Qaraqe, H.-C. Yang, and M.-S. Alouini, "Exact performance analysis of MIMO cognitive radio systems using transmit antenna selection," *IEEE J. Sel. Areas Commun.*, vol. 32, no. 3, pp. 425–438, Mar. 2014.
[16] F. A. Khan, K. Tourki, M.-S. Alouini, and K. A. Qaraqe, "Performance analysis of a power limited spectrum sharing system with TAS/MRC," *IEEE Trans. Signal Process.*, vol. 62, no. 4, pp. 954–967, Feb. 2014.
[17] M. Hanif, H.-C. Yang, and M.-S. Alouini, "Transmit antenna selection for power adaptive underlay cognitive radio with instantaneous interference constraint," *IEEE Trans. Commun.*, vol. 65, no. 6, pp. 2357–2367, Jun. 2017.
[18] R. M. Radaydeh, "SNR and SINR-based selection combining algorithms in the presence of arbitrarily distributed co-channel interferers," *IET Commun.*, vol. 3, no. 1, pp. 57–66, Jan. 2009.
[19] R. M. Radaydeh and M.-S. Alouini, "On the performance of arbitrary transmit selection for threshold-based receive MRC with and without co-channel interference," *IEEE Trans. Commun.*, vol. 59, no. 11, pp. 3177–3191, Nov. 2011.
[20] Y. Huang, F. Al-Qahtani, Q. Wu, C. Zhong, J. Wang, and H. Alnuweiri, "Outage analysis of spectrum sharing relay systems with multiple secondary destinations under primary user's interference," *IEEE Trans. Veh. Technol.*, vol. 63, no. 7, pp. 3456–3464, Sep. 2014.
[21] Y. Huang, F. S. Al-Qahtani, C. Zhong, Q. Wu, J. Wang, and H. M. Alnuweiri, "Cognitive MIMO relaying networks with primary user's interference and outdated channel state information," *IEEE Trans. Commun.*, vol. 62, no. 12, pp. 4241–4254, Dec. 2014.
[22] A. A. AbdelNabi *et al.*, "Performance analysis of MIMO multi-hop system with TAS/MRC in Poisson field of interferers," *IEEE Trans. Commun.*, vol. 64, no. 2, pp. 525–540, Feb. 2016.
[23] A. A. AbdelNabi, F. S. Al-Qahtani, R. M. Radaydeh, and M. Shaqfeh, "Hybrid access femtocells in overlaid MIMO cellular networks with transmit selection under Poisson field interference," *IEEE Trans. Commun.*, vol. 66, no. 1, pp. 163–179, Jan. 2018.
[24] Y. Zou, J. Zhu, B. Zheng, and Y.-D. Yao, "An adaptive cooperation diversity scheme with best-relay selection in cognitive radio networks," *IEEE Trans. Signal Process.*, vol. 58, no. 10, pp. 5438–5445, Oct. 2010.
[25] X. Kang, R. Zhang, Y.-C. Liang, and H. K. Garg, "Optimal power allocation strategies for fading cognitive radio channels with primary user outage constraint," *IEEE J. Sel. Areas Commun.*, vol. 29, no. 2, pp. 374–383, Feb. 2011.
[26] Z. El-Moutaouakkil, K. Tourki, and S. Saoudi, "Spectrally-efficient SIMO relay-aided underlay communications: An exact outage analysis," in *Proc. IEEE Int. Conf. Commun.*, Sydney, NSW, Australia, Jun. 2014, pp. 1531–1536.

[27] X. Gong, A. Ispas, G. Dartmann, and G. Ascheid, "Outage-constrained power allocation in spectrum sharing systems with partial CSI," *IEEE Trans. Commun.*, vol. 62, no. 2, pp. 452–466, Feb. 2014.
[28] Z. El-Moutaouakkil, K. Tourki, and S. Saoudi, "Exact outage analysis of SIMO relay-aided underlay communications with limited feedback," in *Proc. IEEE 83rd Veh. Technol. Conf.*, Nanjing, China, May 2016, pp. 1–7.
[29] J. N. Laneman, D. N. C. Tse, and G. W. Wornell, "Cooperative diversity in wireless networks: Efficient protocols and outage behavior," *IEEE Trans. Inf. Theory*, vol. 50, no. 12, pp. 3062–3080, Dec. 2004.
[30] A. Shah and A. M. Haimovich, "Performance analysis of maximal ratio combining and comparison with optimum combining for mobile radio communications with cochannel interference," *IEEE Trans. Veh. Technol.*, vol. 49, no. 4, pp. 1454–1463, Jul. 2004.
[31] R. K. Mallik, "On multivariate Rayleigh and exponential distributions," *IEEE Trans. Inf. Theory*, vol. 49, no. 6, pp. 1499–1515, Jun. 2003.
[32] R. Tannious and A. Nosratinia, "Spectrally-efficient relay selection with limited feedback," *IEEE J. Sel. Areas Commun.*, vol. 26, no. 8, pp. 1419–1428, Oct. 2008.
[33] N. B. Mehta, S. Kashyap, and A. F. Molisch, "Antenna selection in LTE: From motivation to specification," *IEEE Commun. Mag.*, vol. 50, no. 10, pp. 144–150, Oct. 2012.
[34] P. V. Amadori and C. Masouros, "Large scale antenna selection and precoding for interference exploitation," *IEEE Trans. Commun.*, vol. 65, no. 10, pp. 4529–4542, Oct. 2017.
[35] I. S. Gradshteyn and I. M. Ryzhik, *Table of Integrals, Series and Products*, 7th ed. San Diego, CA, USA: Academic, 2007.
[36] P. S. Bithas, A. A. Rontogiannis, and G. K. Karagiannidis, "An improved threshold-based channel selection scheme for wireless communication systems," *IEEE Trans. Wireless Commun.*, vol. 15, no. 2, pp. 1531–1546, Feb. 2016.
[37] A. P. Prudnikov, Y. A. Brychkov, and O. I. Marichev, *Integrals and Series*. New York, NY, USA: Gordon and Breach Science, 1986.
[38] A. T. McKay, "Sampling from batches," *J. Roy. Stat. Soc.*, vol. 1, no. 2, pp. 207–216, 1934.
[39] *W. Function*. Accessed: 2018. [Online]. Available: http://functions.wolfram.com/HypergeometricFunctions/HypergeometricU/
[40] P. S. Bithas, A. G. Kanatas, D. B. da Costa, P. K. Upadhyay, and U. S. Dias, "On the double-generalized gamma statistics and their application to the performance analysis of V2V communications," *IEEE Trans. Commun.*, vol. 66, no. 1, pp. 448–460, Jan. 2018.

ZAKARIA EL-MOUTAOUAKKIL (M'09) received the Engineer of State Diploma from the Institut National des Postes et Telecommunications, Rabat, Morocco, in 2008. He is currently pursuing the Ph.D. degree with the IMT Atlantique (Telecom Bretagne), Brest, France. From 2008 to 2011, he held various positions in the telecommunications industry with MobiNetS, Nokia Siemens Networks, Sicotel Engineering and Management, and Exceliacom Solutions. His current research interests include virtual MIMO systems, cognitive radio, cooperative relaying, and low-complexity energy/spectrum-efficient algorithms for future mobile and wireless communication networks.

KAMEL TOURKI (SM'13) was born in Antibes, France. He received the Engineering degree in telecommunications from the National School of Engineers of Tunis, Tunisia, in 2003, and the master's and Ph.D. degrees from the University of Nice Sophia-Antipolis, France, in 2004 and 2008, respectively. He is currently a Senior Research Engineer with the Huawei France Research Center. His current research interests include the fields of 4G/5G wireless communication systems, cognitive and cooperative communications, physical layer security, and energy harvesting. He received twice the Research Fellow Excellence Award from TAMUQ (in 2011 and 2014), the Best Poster Award in the IEEE DysPan 2012 Conference, the Outstanding Young Researcher Award from the IEEE Communications Society for Europe-Middle East-Africa Region in 2013. He currently serves as an Editor for the IEEE TRANSACTIONS ON COMMUNICATIONS and the IEEE COMMUNICATIONS LETTERS.

HALIM YANIKOMEROGLU (F'17) is a Full Professor with the Department of Systems and Computer Engineering, Carleton University, Ottawa, ON, Canada. His research interests include many aspects of 5G/5G+ wireless networks, including layers 1–3 and the systems architecture. His collaborative research with industry has resulted in about 30 patents (granted and applied). He is a Distinguished Lecturer for the IEEE Communications Society and a Distinguished Speaker for the IEEE Vehicular Technology Society.

SAMIR SAOUDI (SM'09) was born in Rabat, Morocco, in 1963. He received the Electrical Engineering degree from ENST-Bretagne in 1987, the Ph.D. degree in telecommunications from Rennes I University in 1990, and the HDR Qualification degree as a Supervisor for Ph.D. students in 1997. He was with Orange Laboratory as an Industrial Partner. Since 1991, he has been with the Signal Communications Department, IMT Atlantique (Telecom Bretagne) where he is currently a Professor. He has co-authored over 27 journal papers and one hundred conference papers. His research interests are speech and audio coding, nonparametric probability density estimation, CDMA techniques, multi user detection, MIMO systems, equalization and iterative processing with applications to mobile radio communications. His teaching interests are signal processing, probability, stochastic processes, speech processing and multi user detection for radio communication systems. Since 1995, he has been the Head of the Master Digital Communications Systems. He has supervised over 27 Ph.D. Students. He has been the General Chair of the second International symposium on Image/Video Communications over fixed and mobile networks, in 2004. He has been the Co-Chair of the MIMO Systems Symposium, the IEEE International Wireless Communications and Mobile Computing Conference, IWCMC 2010, France. Since 2008, he has been the Head of the Digital Communications Group, LabSticc, CNRS UMR 6385. Since 2014, he has been the Head of the Signal Communications Department, IMT Atlantique (54 members).